Preparation and Properties of Carbonyliron Complexes of 1-Aza-4-oxa-1,3-butadiene (α-Imino Ester). X-ray Crystal Structures of $Fe(CO)_2(\sigma(N)$: $\sigma(C)$-*i*-PrN(H)C(H)C(O)OEt)$_2$ and $Fe(CO)_2(\sigma(N)$: $\sigma(C)$-*i*-PrN(H)C(H)C(O)OMe)(*i*-PrN=C(H)C(O)O)

Ron Siebenlist, Hans-Werner Frühauf,*,† and Kees Vrieze

Inorganic Laboratory, Institute of Molecular Chemistry, University of Amsterdam, Nieuwe Achtergracht 166, 1018 WV Amsterdam, The Netherlands

Huub Kooijman, Wilberth J. J. Smeets, and Anthony L. Spek*

Bijvoet Center for Bimolecular Research, Crystal and Structural Chemistry, Utrecht University, Padualaan 8, 3584 CH Utrecht, The Netherlands

Received December 22, 1999

Reaction of $Fe_2(CO)_9$ at room temperature in THF or toluene with the α-imino esters (L) $R^1N{=}C(R^2)C(R^3){=}O$ (**a**−**i**; R^1 = alkyl, R^2 = H, R^3 = *O*-alkyl), results in the formation of several mono- and binuclear complexes, depending on the bulkiness of the R^1 substituent. With all ligands employed, the known type of complex $Fe_2(CO)_6(L)$ (**6**) is formed. Reaction of the less bulky R^1 substituted ligands **a**−**e** (R^1 = *neo*-Pe, *i*-Pr, 1-cyclohexylethyl) leads to the formation of $Fe(CO)_2(\sigma(N)$: $\sigma(C)$-*i*-PrN(H)C(H)C(O)OEt)$_2$ (**10a**−**d/10′a**−**d**) as a mixture of two noninterconverting isomers together with the known type of complexes $Fe_2(CO)_6(L{-}L)$ (**7**). Complexes **7** contain two (former) α-imino ester ligands joined at the imine carbon atoms. In the presence of water, the reaction in THF leads to the formation of $Fe(CO)_2(\sigma(N)$: $\sigma(C)$-*i*-PrN(H)C(H)C(O)OMe)(*i*-PrN=C(H)C(O)O) (**11/11′**). The unusual σ(N):σ(C) coordination of the newly formed ligands in **10** and **11** is confirmed by X-ray structure determinations. Thermal or photochemical activation of **7** in toluene leads to the formation of $Fe_2(CO)_4(L{-}L)$ (**9**), and reaction of **7** with HCl leads to displacement of the N-protonated C−C coupled organic compounds **8**. Reaction of **9** with CO (1 atm) at room temperature results in the re-formation of **7**. Reaction with the bulky substituted R^1 ligands **f**−**i** (R^1 = *t*-Bu, 2-methyl-2-butyl) results in the formation of the new binuclear complexes $Fe_2(CO)_5(L{-}L)$ (**12**) in which, like in **7**, two α-imino ester ligands are C−C coupled on the imine carbon atoms. In contrast to **7**, the C=O oxygen atoms in **12** are coordinated, and instead of a metal−metal bond a bridging CO is present. All complexes and the organic products have been characterized by spectroscopy (IR, ^{1}H and ^{13}C NMR, FD/FAB-mass) and by elemental analyses. An explanation for the product distribution and the possible mechanisms for the formation of the complexes is discussed.

Introduction

α-Diimine ligands $R^1N{=}CHCH{=}NR^1$ (R-DAB)[1] and C_6H_4N-2-$CH{=}NR^1$ (R-Pyca)[1] in transition-metal complexes are known for their versatile coordination behavior, based on their ability to donate from two up to eight electrons via the nitrogen lone pairs and the C=N π-electrons toward one or more metal centers.[2−6] Reaction of these ligands with metal carbonyls, especially of group 8, leads to the formation of several mono-, di-, and polynuclear complexes.[2−7] An interesting aspect of the versatile coordination chemistry is the activation of the imine carbon atoms toward C−C,[7−10] C−H,[11−13] C−N,[12−14] and N−H[15] coupling reactions of R-DAB ligands in the coordination sphere of transi-

† E-mail: hwf@anorg.chem.uva.nl. Fax: +31-20-525 6456.

(1) The abbreviations used throughout this text are as follows: R-DAB, 1,4-diaza-1,3-butadienes of formula $R^1N{=}C(H)C(H){=}NR^1$; R-Pyca, 1,4-diaza-1,3-butadienes of formula C_5H_4N-2-$(C(H){=}NR^1)$; DMAD, dimethyl acetylenedicarboxylate; MP, methyl propynoate; CE, 1-cyclohexylethyl; *t*-Am, 2-methyl-2-butyl; R-ADO, 1,6-di-R-1,6-diazahexa-1,5-diene-3,4-dimethyl-3,4-diolato, $R^1N{=}C(H)(Me)C(O)(H)C(O)C(Me){=}NR^1$; R^1,R^3-ODA, 1,6-dioxahexa-1,5-diene-2,5-di-R^3-3,4-di-R^1-aminato, $O{=}C(R^3)(H)C(NR^1)(H)C(NR^1)C(R^3){=}O$; R-ADA, 1,6-di-R-1,6-diazahexa-1,5-diene-3,4-di-R-aminato, the reductively C−C coupled dimer of R-DAB, $R^1N{=}C(H)(H)C(NR^1)(H)C(NR^1)C(H){=}NR^1$; R-APE, 1,2-di-R-aminato-1,2-bis(2-pyridyl)ethane, the reductively C−C coupled dimer of R-Pyca, $[C_5H_4N\text{-}2]CH(NR^1)CH(NR^1)\text{-}2\text{-}C_5H_4N$.

(2) Vrieze, K.; van Koten, G. *Inorg. Chim. Acta* **1985**, *100*, 79.
(3) Vrieze, K. *J. Organomet. Chem.* **1986**, *300*, 307.
(4) Zoet, R.; van Koten, G.; Stam, C. H.; Stufkens, D. J.; Vrieze, K. *Organometallics* **1988**, *7*, 2118.
(5) Zoet, R.; Jastrzebski, J. T. B. H.; van Koten, G.; Mahabiersing, T.; Vrieze, K.; Stam, C. H.; Heijdenrijk, D. *Organometallics* **1988**, *7*, 2108.
(6) van Koten, G.; Vrieze, K. *Adv. Organomet. Chem.* **1982**, *21*, 151.
(7) Muller, F.; van Koten, G.; Polm, L. H.; Vrieze, K.; Zoutberg, M. C.; Heijdenrijk, D.; Kragten, E.; Stam, C. H. *Organometallics* **1989**, *8*, 1340.
(8) Polm, L. H.; van Koten, G.; Vrieze, K.; Stam, C. H.; van Tunen, W. C. J. *J. Chem. Soc., Chem. Commun.* **1983**, 1177.

10.1021/om9910266 CCC: $19.00
Publication on Web 07/06/2000

tion metals with a wide variety of molecules such as α-diimines,[9,10,16−18] carbodiimides,[19] sulfines,[19] ketenes,[8] and especially alkynes.[14,20−22]

In a series of previous papers[23−34] we have reported in detail on C−C coupling reactions of the chelate (1,4-diaza-1,3-butadiene)$Fe(CO)_3$ complexes **1** with the electron-deficient alkyne dimethyl acetylenedicarboxylate (DMAD).[1] The initial step in these reactions consists of an oxidative 1,3-dipolar [3 + 2] cycloaddition reaction of the electron-deficient alkyne (dipolarophile) across the Fe−N═C fragment (the 1,3-dipole) to give intermediate **2**. Insertion of CO into the Fe−N bond and subsequent uptake of an additional ligand (L′), followed by reductive elimination and recoordination of the double bond, finally leads to the formation of (1,5-dihydropyrrol-2-one)$Fe(CO)_3$ complexes **3** (cf. Scheme 1; X = NR^1, R^3 = H).

To expand the potential of these organometallic 1,3-dipolar cycloadditions, we also investigated the reactions of the closely related σ(N):σ(O) chelate $Fe(CO)_3(R^1N$═$C(R^2)C(R^3)$═O) (α-imino ketones, X = O, R^3 = Me, Ph;[24,25] α-imino esters, X = O, R^3 = *O*-alkyl[35]) toward DMAD and MP[1] and found an analogous reactivity. During these investigations we found that these ligands show interesting coordination behavior toward iron carbonyl. In contrast to the α-diimine chemistry relatively little is known about the coordination behavior of α-imino ketones and especially esters toward d^8 metals. α-Imino ketones and esters have been shown to form several types of coordination complexes with $Pt(Cl)_2(PR_3)_2$, ZnR_2, AlR_3, $ZnCl_2$, and $AlCl_3$, monodentate *trans*-$[PtCl_2(PEt_3)(R^1N$═$C(R^2)C(R^3)$═O], bridging bidentate $[(AlMe_3)_2$(σ(*N*):σ(*O*)-MeN═C(Ph)C(Ph)═O)],[37] and the dimeric $[EtZn(Et)(t\text{-}Bu)NC(H)$═$C(Me)O]_2$[38] complex. Weiss et al.[39] reported on the reaction of the α-imino ester PhCH(Me)N═C(H)C(OEt)═O (L*) with iron carbonyl, which resulted in the formation of two binuclear products, $Fe_2(CO)_6$(L*) (**6**) and the $Fe_2(CO)_6$(L*−L*) (**7**) complex (cf. Scheme 2), in which the imine-C atoms of two α-imino ketone ligands have been C−C coupled. This C−C coupled ligand will be abbreviated as R^1,R^3-ODA.[1]

Scheme 1. Reactions of $Fe(CO)_3(R^1N$═$C(H)C(R^3)$═X) (X═NR^1, O) with DMAD

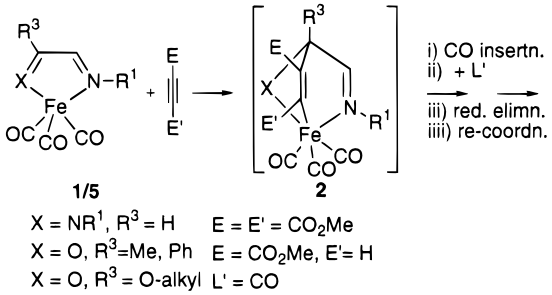

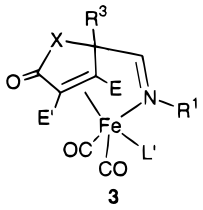

Scheme 2. Reaction of $Fe_2(CO)_9$ with PhCH(Me)N═C(H)C(OEt)═O (L*)

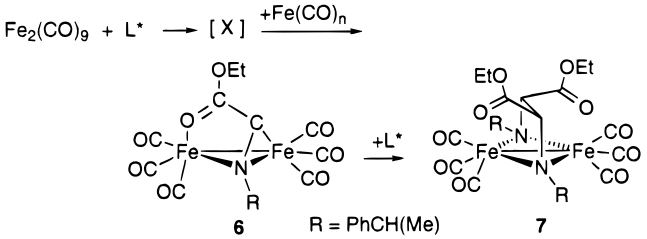

(9) Polm, L. H.; Elsevier, C. J.; van Koten, G.; Ernsting, J. M.; Stufkens, D. J.; Vrieze, K.; Andréa, R. R.; Stam, C. H. *Organometallics* **1987**, *6*, 1096.
(10) Mul, W. P.; Elsevier, C. J.; Frühauf, H.-W.; Vrieze, K.; Pein, I.; Zoutberg, M. C.; Stam, C. H. *Inorg. Chem.* **1990**, *7*, 2336.
(11) Zoet, R.; van Wijnkoop, M.; Versloot, P.; van Koten, G.; Vrieze, K.; Duineveld, C. A. A.; Elsevier, C. J.; Goubitz, K.; Heijdenrijk, D.; Stam, C. H. *Organometallics* **1989**, *8*, 23.
(12) Muller, F.; van Koten, G.; Vrieze, K.; Heijdenrijk, D.; Krijnen, B. B.; Stam, C. H. *Organometallics* **1989**, *8*, 41.
(13) Muller, F.; van Koten, G.; Vrieze, K.; Duineveld, K. A. A.; Heijdenrijk, D.; Mak, A. N. S.; Stam, C. H. *Organometallics* **1989**, *8*, 1324.
(14) Muller, F.; van Koten, G.; Vrieze, K.; Heijdenrijk, D. *Organometallics* **1989**, *8*, 33.
(15) Keijsper, K.; Mul, J.; van Koten, G.; Vrieze, K.; Ubbels, H. C.; Stam, C. H. *Organometallics* **1984**, *3*, 1732.
(16) Staal, L. H.; Polm, L.; Balk, R. W.; van Koten, G.; Vrieze, K.; Brouwer, A. M. F. *Inorg. Chem.* **1980**, *19*, 3343.
(17) Keijsper, J.; van Koten, G.; Vrieze, K.; Zoutberg, M. C.; Stam, C. H. *Organometallics* **1985**, *4*, 1306.
(18) Keijsper, J.; Polm, L. H.; van Koten, G.; Vrieze, K.; Abbel, G.; Stam, C. H. *Inorg. Chem.* **1984**, *23*, 2142.
(19) Keijsper, J.; Polm, L. H.; van Koten, G.; Vrieze, K.; Stam, C. H.; Schagen, J. D. *Inorg. Chim. Acta* **1985**, *103*, 137.
(20) Muller, F.; van Koten, G.; Kraakman, M. J. A.; Vrieze, K.; Zoet, R.; Duineveld, K. A. A.; Heijdenrijk, D.; Stam, C. H.; Zoutberg, M. C. *Organometallics* **1989**, *8*, 982.
(21) Muller, F.; van Koten, G.; Kraakman, M. J. A.; Vrieze, K.; Heijdenrijk, D.; Zoutberg, M. C. *Organometallics* **1989**, *8*, 1331.
(22) Muller, F.; Dijkhuis, D. I. P.; van Koten, G.; Vrieze, K.; Heijdenrijk, D.; Rotteveel, M. A.; Stam, C. H.; Zoutberg, M. C. *Inorg. Chim. Acta* **1989**, *158*, 99.
(23) van Wijnkoop, M.; de Lange, P. P. M.; Frühauf, H.-W.; Vrieze, K.; Wang, Y.; Goubitz, K.; Stam, C. H. *Organometallics* **1992**, *11*, 3607.
(24) van Wijnkoop, M.; Siebenlist, R.; Ernsting, J. M.; de Lange, P. P. M.; Frühauf, H.-W.; Horn, E.; Spek, A. L. *J. Organomet. Chem.* **1993**, *482*, 99.
(25) van Wijnkoop, M.; Siebenlist, R.; de Lange, P. P. M.; Frühauf, H.-W.; Vrieze, K.; Smeets, W. J. J.; Spek, A. L. *Organometallics* **1993**, *12*, 4172.
(26) Frühauf, H.-W.; Seils, F.; Goddard, R. J.; Romão, M. J. *Angew. Chem., Int. Ed. Engl.* **1983**, *22*, 992.
(27) Frühauf, H.-W.; Seils, F.; Goddard, R. J.; Romão, M. J. *Organometallics* **1985**, *4*, 948.
(28) Frühauf, H.-W. *J. Organomet. Chem.* **1986**, *302*, 59.
(29) Frühauf, H.-W.; Seils, F. *J. Organomet. Chem.* **1987**, *323*, 67.
(30) Frühauf, H.-W.; Seils, F.; Stam, C. H. *Organometallics* **1989**, *8*, 2338.
(31) de Lange, P. P. M.; Frühauf, H.-W.; van Wijnkoop, M.; Kraakman, M. J. A.; Kranenburg, M.; Groot, A. H. J. P.; Fraanje, J.; Wang, Y.; Numan, M. *Organometallics* **1993**, *12*, 417.
(32) de Lange, P. P. M.; van Wijnkoop, M.; Frühauf, H.-W.; Vrieze, K.; Goubitz, K. *Organometallics* **1993**, *12*, 428.
(33) de Lange, P. P. M.; de Boer, R. P.; van Wijnkoop, M.; Ernsting, J. M.; Frühauf, H.-W.; Vrieze, K.; Smeets, W. J. J.; Spek, A. L. *Organometallics* **1993**, *12*, 440.
(34) de Lange, P. P. M.; Alberts, E.; van Wijnkoop, M.; Frühauf, H.-W.; Vrieze, K.; Kooijman, H.; Spek, A. L. *J. Organomet. Chem.* **1994**, *465*, 241.
(35) Siebenlist, R.; de Beurs, M.; Feiken, N.; Frühauf, H.-W.; Vrieze, K.; Kooijman, H.; Veldman, N.; Spek, A. L. *Organometallics* **2000**, *19*, 3032−3053.
(36) van Vliet, M. R. P.; van Koten, G.; van Beek, J. A. M.; Vrieze, K.; Muller, F.; Stam, C. H. *Inorg. Chem. Acta* **1986**, *112*, 77.
(37) van Vliet, M. R. P.; van Koten, G.; Rotteveel, M. A.; Scharp, M.; Vrieze, K.; Kojic-Prodic, B.; Spek, A. L.; Duisenberg, A. J. M. *Organometallics* **1986**, *5*, 1389.
(38) van Vliet, M. R. P.; van Koten, G.; Buysingh, P.; Jastrzebski, J. T. B. H.; Spek, A. L. *Organometallics* **1987**, *6*, 537.
(39) de Cian, A.; Weiss, R. E.; Chauvin, Y.; Commereuc, D.; Hugo, D. *J. Chem. Soc. Chem. Commun.* **1976**, 249.

Scheme 3. Observed Reactions of the α-Imino Esters a−i with $Fe_2(CO)_9$

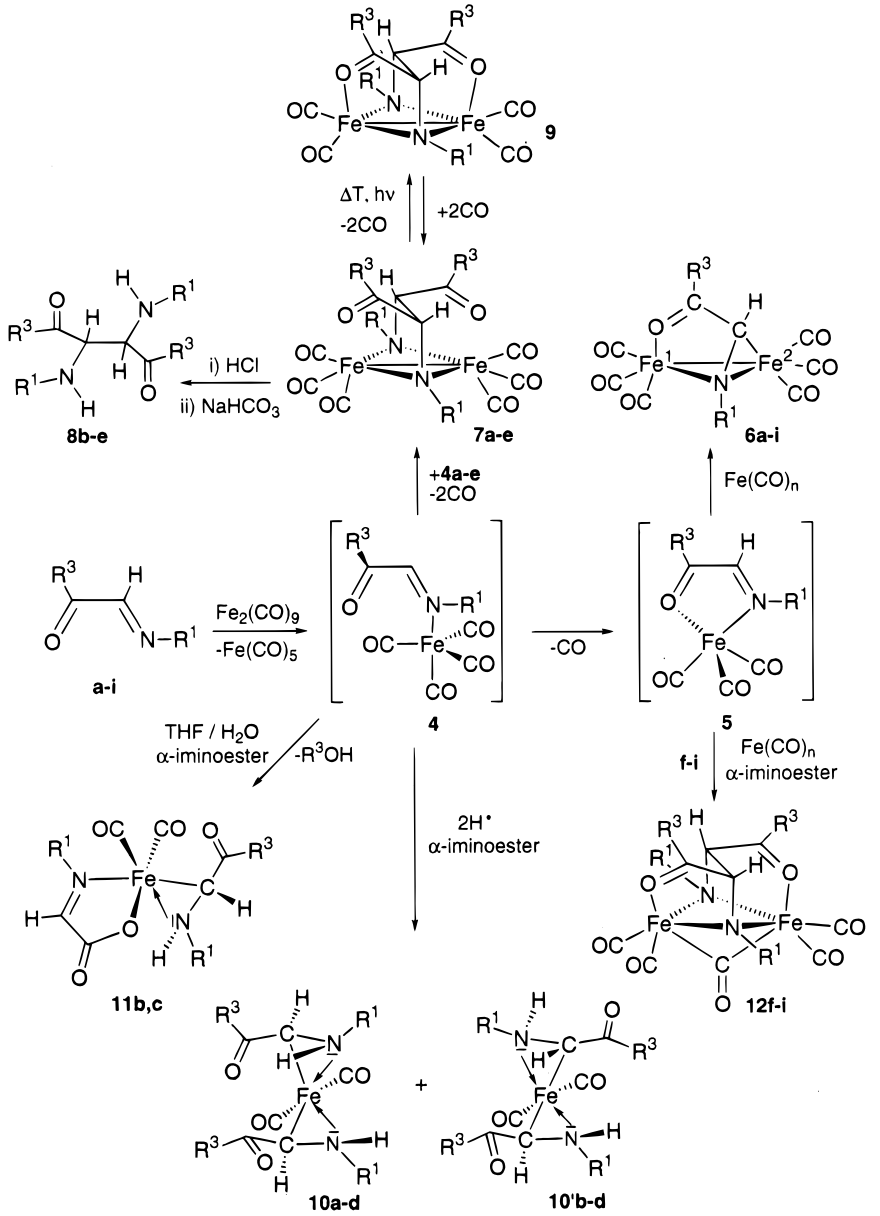

Recently, we reported on the coordination chemistry of α-imino ketones toward iron carbonyl[40] leading to $Fe(CO)_3$(α-iminoketone), $Fe_2(CO)_6$(α-imino ketone), and $Fe_2(CO)_4$(R-ADO).[1] In the last complex a type of C−C coupled ligand similar to that in **7** is formed; however, in $Fe_2(CO)_4$(R-ADO) the C−C coupling has occurred between the two ketone carbon atoms of the α-imino ketone instead of the imine carbons.

In this article we report on an investigation of the reactions of α-imino esters $R^1N{=}C(H)C(R^3){=}O$ (R^1 = alkyl, R^2 = H, R^3 = *O*-alkyl; **a**−**i**) with $Fe_2(CO)_9$, resulting in the formation of the two new mononuclear complexes **10a**−**d/10′a**−**d** and **11b**,**c/11′b**,**c** and the new C−C coupled dimeric complexes $Fe_2(CO)_5(R,R^3\text{-ODA})$[1] (**12f**−**i**) together with the known types of complexes **6a**−**i** and **7a**−**e**[39] (cf. Scheme 3). The product selectivity strongly depends on the imine R^1 substituent and on the solvent. An explanation for this and the possible mechanisms for the formation of the complexes will be discussed.

Experimental Section

General Remarks. ^1H and ^{13}C NMR spectra were recorded on a Bruker AMX-300 spectrometer. IR spectra were recorded on Perkin-Elmer 283 and Biorad FTIR-7 spectrophotometers. Elemental analyses were carried out by Dornis & Kolbe, Microanalytisches Laboratorium, Mülheim a. d. Ruhr, Germany. The solvents were carefully dried and distilled under nitrogen before use. All preparations were carried out under an atmosphere of dry nitrogen by standard Schlenk techniques. The irradiations were carried out using the 514.5 nm line of a SP 2025 argon ion laser or a Philips HPK 125 W high-pressure mercury lamp equipped with the appropriate interference filter. Silica gel for column chromatography (Kieselgel 60, 70−230 mesh, E. Merck, Darmstadt, Germany) was dried and activated prior to use by heating to 180 °C under vacuum for 16 h. $Fe(CO)_5$ (Strem Chemicals) and dimethyl, diethyl, and diisopropyl L-tartrates (Aldrich) were used as commercially obtained.

Synthesis of Starting Materials. $Fe_2(CO)_9$[41] and the

(40) Siebenlist, R.; Frühauf, H.-W.; Vrieze, K.; Smeets, W. J. J.; Spek, A. L. *Eur. J. Inorg. Chem*., in press.

Table 1. Syntheses of Complexes 6a−i, 7a−e, 10a−d/10′a−d, 11b,c/11′b,c, and 12f−i

	ligand substituents						
compd	R^1	R^3	amt of ligand (mmol)[a]	amt of $Fe_2(CO)_9$ (g (mmol))	elution ratio[b]	yield[c] (%)	yield[d] (%)
6a	*neo*-Pe	OMe	3.18	2.31 (6.36)	15:1	16	13
6b	*i*-Pr	OMe	3.87	2.82 (7.74)	15:1	13	11
6c	*i*-Pr	OEt	3.49	2.54 (6.98)	15:1	13	11
6d	*i*-Pr	O-*i*-Pr	3.18	2.31 (6.36)	15:1	10	10
6e/6′e[e]	CE	OMe	2.53	1.84 (5.06)	15:1	10	11
6f	*t*-Bu	OMe	3.49	2.54 (6.98)	9:1	10	10
6g	*t*-Bu	OEt	3.18	2.31 (6.36)	9:1	7	11
6h	*t*-Bu	O-*i*-Pr	2.92	2.13 (5.84)	9:1	7	9
6i	*t*-Am	OMe	3.18	2.31 (6.36)	9:1	10	10
7a	*neo*-Pe	OMe	3.18	2.31 (6.36)	9:1	23	4
7b	*i*-Pr	OMe	3.87	2.82 (7.74)	9:1	24	5
7c	*i*-Pr	OEt	3.49	2.54 (6.98)	9:1	26	5
7d	*i*-Pr	O-*i*-Pr	3.18	2.31 (6.36)	9:1	24	5
7e	CE	OMe	2.53	1.84 (5.06)	9:1	23	
10′a	*neo*-Pe	OMe	3.18	1.15 (3.18)	1:1		10
10b/10′b[e]	*i*-Pr	OMe	3.87	1.41 (3.87)	1:1	3	12
10c/10′c[e]	*i*-Pr	OEt	3.49	1.27 (3.49)	1:1	3	12
10d/10′d[e]	*i*-Pr	O-*i*-Pr	3.18	1.15 (3.18)	1:1	3	13
11b	*i*-Pr	OMe	3.87	1.41 (3.87)			14
11c	*i*-Pr	OEt	3.49	1.27 (3.49)			20
12f	*t*-Bu	OMe	3.49	2.54 (6.98)	3:1	32	12
12g	*t*-Bu	OEt	3.18	2.31 (6.36)	3:1	33	12
12h	*t*-Bu	O-*i*-Pr	2.92	2.13 (5.84)	5:1	38	9
12i	*t*-Am	OMe	3.18	2.31 (6.36)	3:1	32	11
12fg	*t*-Bu	OMe/Et		2.31 (6.36)	3:1		

[a] On the basis of 0.5 g of the respective α-imino ketone. [b] Ratio of pentane to Et_2O for elution of **6**, **7**, and **10**; ratio of Et_2O to CH_2Cl_2 for the elution of **12**. [c] Yield in toluene. [d] Yield in THF. [e] Ratios of isomers: **6e**:**6e′** (3:1); **10**:**10′** (6:1); **11**:**11′** (15:1).

α-imino esters **b**, **c**, **f**, and **g** have been prepared according to published procedures.[42]

The new α-imino esters $R^1N{=}C(H)C(OMe){=}O$ with R^1 = neopentyl (*neo*-Pe; **a**), 1-cyclohexylethyl (CE; **e**), 2-methyl-2-butyl (*t*-Am;[1] **i**) and $R^1N{=}C(H)C(O\textit{i}\text{-Pr}){=}O$ with R^1 = *i*-Pr (**d**), *t*-Bu (**h**) were synthesized by reaction of methyl or isopropyl glyoxylate,[43] respectively, with the corresponding amines according to ref 42. Yield: **a**, 30%; **d**, 50%; **e**, 70%; **h**, 70%; **i**, 70%.

IR (ν_{max} in pentane, cm^{-1}): **a**, 1761 m, 1735 s $\nu(CO_2Me)$, 1653 w $\nu(C{=}N)$; **b**, 1765 m, 1739 s $\nu(CO_2Me)$, 1652 w $\nu(C{=}N)$; **c**, 1761 m, 1730 s $\nu(CO_2Me)$, 1652 w $\nu(C{=}N)$; **d**, 1757 m, 1725 s $\nu(CO_2Me)$, 1652 w $\nu(C{=}N)$; **e**, 1766 m, 1738 s $\nu(CO_2Me)$, 1652 w $\nu(C{=}N)$; **f**, 1761 m, 1738 s $\nu(CO_2Me)$, 1652 w $\nu(C{=}N)$; **g**, 1762 m, 1728 s $\nu(CO_2Me)$, 1653 w $\nu(C{=}N)$; **h**, 1751 m, 1724 s $\nu(CO_2Me)$, 1652 w $\nu(C{=}N)$; **i**, 1766 m, 1735 s $\nu(CO_2Me)$, 1652 w $\nu(C{=}N)$.

^{1}H NMR (300.13 MHz, $CDCl_3$, room temperature, δ in ppm relative to TMS): **a**, 7.65 (t, 1H, 1.3 Hz, N=C*H*), 3.86 (s, 3H, OCH_3), 3.39 (d, 2H, 1.3 Hz, CH_2C$(CH_3)_3$), 0.95 (s, 9H, C(C$H_3)_3$); **d**, 7.70 (s, 1H, N=C*H*), 5.20 (sept, 1H, 6.3 Hz, OC*H*$(CH_3)_2$), 3.61 (sept, 1H, 6.3 Hz, NC*H*$(CH_3)_2$), 1.34, 1.27 (2 × d, 12H, 6.3 Hz, 2 × CH(C$H_3)_2$); **e**, 7.63 (s, 1H, N=C*H*), 3.87 (s, 3H, OCH_3), 3.03 (dq, 1H, 6.8 Hz, NC*H*), 1.81−1.41 (m, 6H, *c*-Hex *H*), 1.32−1.02 (m, 3H, *c*-Hex *H*), 1.21 (d, 3H, 6.4 Hz, NCCH_3), 0.96−0.72 (m, 2H, *c*-Hex *H*); **h**, 7.64 (s, 1H, N=C*H*), 5.20 (sept, 1H, 6.3 Hz, C*H*$(CH_3)_2$), 1.34 (d, 6H, 6.3 Hz, CH(C$H_3)_2$), 1.28 (s, 9H, C(C$H_3)_3$); **i**, 7.60 (s, 1H, N=C*H*), 3.87 (s, 3H, OCH_3), 1.63 (q, 2H, 7.5 Hz, CH_2CH$_3$), 1.20 (s, 6H, C(C$H_3)_2$), 0.77 (t, 3H, 7.5 Hz, CH$_2$CH_3).

^{13}C NMR (75.47 MHz, $CDCl_3$, room temperature, δ in ppm relative to TMS): **a**, 163.2 (C=O), 151.0 (C=N), 71.8 (NCH_2), 53.1 (OCH_3), 33.1 (*C*$(CH_3)_3$), 28.2 (C(*C*$H_3)_3$), **d**, 161.5 (C=O), 150.6 (C=N), 67.9 (O*C*H$(CH_3)_2$), 60.5 (N*C*H$(CH_3)_2$), 27.8 (OCH-(*C*$H_3)_2$), 21.9 (NCH(*C*$H_3)_2$), **e**, 164.1 (C=O), 153.8 (C=N), 75.6 (N*C*CH$_3$), 52.1 (O*C*H$_3$), 42.7 (*c*-Hex *C*H), 29.7, 29.2, 26.2, 26.0, 25.8 (*c*-Hex *C*H$_2$), 19.1(NC*C*H$_3$); **h**, 161.4 (C=O), 147.6 (C=N), 67.2 (O*C*H$(CH_3)_2$), 57.6 (*C*$(CH_3)_3$), 27.8 (OCH(*C*$H_3)_2$), 20.5 (C(*C*$H_3)_3$); **i**, 163.0 (C=O), 148.0 (C=N), 60.7 (N*C*), 51.3 (O*C*H$_3$), 34.2 (C(*C*$H_3)_2$), 25.1 (*C*H$_2$CH$_3$), 7.5 (CH$_2$*C*H$_3$).

Synthesis of Complexes. The general procedures for the preparation of complexes **6a**−**i**, **7a**−**e**, **10a**−**d**/**10′a**−**d**, **11b**,**c**/**11′b**,**c**, and **12f**−**i** are given below; details are listed in Table 1.

Synthesis of $Fe_2(CO)_6$(L) (6a−e) and $Fe_2(CO)_6$(R^1,R^3-ODA) (7a−e). To a stirred suspension of $Fe_2(CO)_9$ in 50 mL of toluene was added 0.5 g of the respective α-imino ester (cf. Table 1), whereupon the solution turned dark purple. The reaction mixture was stirred for 16 h, during which time the color of the reaction mixture changed from deep purple to red-brown. The reaction mixture was evaporated to dryness, the residue was redissolved in a minimum of CH_2Cl_2, and the products were separated by column chromatography on silica gel (column 1 × 20 cm). Elution with pentane afforded a green fraction, containing $Fe_3(CO)_{12}$. Further elution with pentane/Et_2O afforded a brown-orange fraction which after evaporation of the solvent gave $Fe_2(CO)_6$(L) (**6a**−**e**) as an orange-brown oil. Crystallization from pentane at −60 °C resulted in most cases in red-brown crystalline products; the yields varied between 10 and 16% (isolated product) depending on the ligand used. Continued elution with pentane/Et_2O afforded an orange to yellow fraction which after evaporation of the solvent gave $Fe_2(CO)_6$(R^1,R^3-ODA) (**7a**−**e**) as a yellow powder in 23−26% yield depending on the ligand used. Analytically pure complexes could be obtained by crystallization from pentane or pentane/Et_2O (10:1) at −60 °C, resulting in orange to orange-brown crystals in almost quantitative yield.

Synthesis of $Fe_2(CO)_6$(L) (6f−i) and $Fe_2(CO)_5$(R^1,R^3-ODA) (12f−i). (a) Reaction in Toluene. To a stirred suspension of $Fe_2(CO)_9$ in 50 mL of toluene, 0.5 g of the respective α-imino ester was added (cf. Table 1), whereupon

(41) $Fe_2(CO)_9$ was prepared by a slightly modified literature procedure (Braye, E. H.; Hübel, W. *Inorg. Synth.* **1966**, *8*, 178) using a quartz Schlenk tube and starting with 25 mL of $Fe(CO)_5$, 150 mL of glacial acetic acid, and 10 mL of acetic anhydride (the last compound was added to prevent the mixture from containing too much water). A Rayonet RS photochemical reactor (λ_{max} = 2500 Å) was used for irradiation, and a continuous stream of air was used to cool the reaction mixture. Filtering, washing with water, ethanol, and ether, and subsequently drying in vacuo gave $Fe_2(CO)_9$ in usually more than 90% yield.

(42) van der Poel, H.; van Koten, G. *Synth. Commun.* **1978**, *8*, 305.

(43) Kelly, R. T.; Schimdt, T. E.; Haggerty, J. G. *Synthesis* **1972**, 544.

the solution turned dark blue. The reaction mixture was stirred for 16 h, during which time the color of the reaction mixture changed from deep blue to red-brown. The reaction mixture was evaporated to dryness, the residue was redissolved in a minimum of CH_2Cl_2, and the products were separated by column chromatography on silica gel (column 1 × 20 cm). Elution with pentane afforded a green fraction, containing $Fe_3(CO)_{12}$. Further elution with pentane/Et_2O afforded a brown-orange fraction which after evaporation of the solvent gave $Fe_2(CO)_6(L)$ (**6f**−**i**) as a brown oil. Crystallization from pentane at −80 °C resulted in most cases in red-brown crystalline products, in yields of 7−10% (isolated product) depending on the ligand used. Subsequent elution with Et_2O/CH_2Cl_2 afforded a dark blue fraction which after evaporation of the solvent yielded $Fe_2(CO)_5(R^1,R^3\text{-ODA})$ (**12f**−**i**) as a blue powder in 32−38% yield. Crystallization from Et_2O/CH_2Cl_2 (4:1) resulted in dark purple-blue diamond-shaped crystals of **12f**−**h**, which due to twinning were unsuitable for determination of refined structures by X-ray diffraction. Crystallization of **12i** yielded a dark blue crystalline powder. Reaction of equimolar quantities of ligands **f** and **g** resulted in formation of the mixed Me/Et substituted complex **12fg**. Crystallization resulted in purple-blue diamond-shaped crystals of **12fg**, which were unfortunately again not suitable for X-ray diffraction.

(b) Reaction in THF. The reaction in THF was performed as in toluene, only for 3 instead of 16 h. The yields of **6f**−**i** varied from 9 to 11% and the yields for **12f**−**i** between 9 and 12%.

Synthesis of $Fe(CO)_2(\sigma(N)\text{:}\sigma(C)\text{-}R^1NC(H)CR^3)_2$ (10a−d/10′a−d). To a stirred suspension of $Fe_2(CO)_9$ in 25 mL of THF was added 0.5 g of the respective α-imino ester (cf. Table 1), whereupon the solution turned dark purple. The reaction mixture was stirred for 3 h, during which time the color of the reaction mixture changed from deep purple to red-brown. The reaction mixture was evaporated to dryness, the residue was redissolved in a minimum of CH_2Cl_2, and the products were separated by column chromatography on silica gel (column 1 × 15 cm). Elution with pentane afforded a green fraction, containing $Fe_3(CO)_{12}$. Further elution with pentane/Et_2O (4:1) afforded a red-brown fraction containing small amounts of $Fe_2(CO)_6(L)$ (**6**) and $Fe_2(CO)_6(R^1,R^3\text{-ODA})$ (**7**). Subsequent elution with Et_2O afforded a yellow to brown fraction. This fraction was evaporated to dryness and rechromatographed because the brown oily residue still contained impurities. Elution with pentane/Et_2O (5:1) afforded a small orange fraction containing traces of $Fe_2(CO)_6(R^1,R^3\text{-ODA})$ (**7**). Subsequent elution with pentane/Et_2O (1:1) afforded one yellow fraction for **10a** and **10b/10′b**. For **10c**,**d/10′c**,**d** two separate yellow fractions were collected; the first fraction contained pure **10′c**,**d** and the second fraction contained almost pure **10c**,**d**. The ratio of **10b**−**d** to **10′b**−**d** was approximately 1:6. After evaporation of the solvent **10a**−**d/10′a**−**d** were isolated as yellow powders in 10−13% yield. Analytically pure complexes were obtained by crystallization from pentane or pentane/CH_2Cl_2 (10:1), resulting in yellow to yellow-orange crystals. Crystals of **10c** were suitable for X-ray diffraction.

Synthesis of $Fe(CO)_2(\sigma(N)\text{:}\sigma(C)\text{-}i\text{-}PrNC(H)CR^3)(R^1N{=}C(H)C(O)O)$ (11b,c). To a stirred suspension of $Fe_2(CO)_9$ in 15 mL of THF were added 0.5 g of the respective α-imino ester and 3 equiv of H_2O (cf. Table 1), whereupon the solution turned deep purple. The reaction mixture was stirred for 5 h, during which time the color of the reaction mixture changed from deep purple to red-brown. The reaction mixture was evaporated to dryness, the residue was redissolved in a minimum of CH_2Cl_2, and the products were separated by column chromatography on silica gel (column 1 × 15 cm). Elution with Et_2O afforded a red-brown fraction, containing traces of $Fe_2(CO)_6(L)$ (**6b,c**) and $Fe_2(CO)_6(R^1,R^3\text{-ODA})$ (**7b,c**). Elution with CH_2Cl_2 yielded a fraction containing unknown paramagnetic products. Subsequent elution with CH_2Cl_2/THF (1:1) afforded a yellow-brown fraction which after evaporation of the solvent gave **11b**,**c/11′b**,**c** as yellow powders in 14 and 17% yields, respectively. Analytically pure complexes were obtained by crystallization from Et_2O/CH_2Cl_2 (5:1), resulting in yellow to yellow-brown crystals. Crystals of **11b** were suitable for X-ray diffraction.

Reaction of $Fe_2(CO)_6(R^1,R^3\text{-ODA})$ (7b−e) with HCl. To a solution of 200 mg of $Fe_2(CO)_6(R^1,R^3\text{-ODA})$ (**7b**−**e**) in 40 mL of toluene was added 5 mL of concentrated aqueous HCl. When the organic layer had become colorless, after about 2−4 days, the excess of HCl was neutralized with $NaHCO_3$. The aqueous layer was separated and extracted twice with 50 mL of Et_2O. The combined organic layers were dried (Na_2SO_4) and evaporated to dryness, the residue was redissolved in pentane, and this solution was purified by column chromatography on silica gel (column 1 × 15 cm). Elution with pentane/Et_2O (3:1) afforded a colorless fraction, which after evaporation of the solvent gave **8b**−**e** as colorless oils in 70% yield. Analytically pure **8e** was obtained by crystallization from pentane at −80 °C, resulting in white crystalline material in 50% yield.

Thermal and Photochemical Conversion of 7b−d to $Fe_2(CO)_4(R^1,R^3\text{-ODA})$ (9b−d). Thermolysis. When a solution of 100 mg of $Fe_2(CO)_6(R^1,R^3\text{-ODA})$ (**7b**−**d**) in toluene (20 mL) was stirred at reflux, the color of the solution changed from orange to deep green. The reaction was followed by IR spectroscopy and revealed that a new product was formed with CO stretching bands at about 1999, 1950, 1911, and 1665 cm^{-1}. The reaction was stopped (±3 h) when the intensities of the IR bands of **9** were at their maximum, at which time approximately 70−80% of **7b**−**d** was consumed. Prolonged heating did not improve the yields of **9**. After evaporation of the solvent the green/brown residue was dissolved in 10 mL of Et_2O. The resulting deep green solution was filtered and gave after evaporation of the solvent a green oily residue containing a 2:3 mixture of **7** and **9**. Unfortunately, due to decomposition of **9** on silica no further purification was possible. Complex **9b** has been characterized by IR, ^1H and ^{13}C NMR, and UV−vis spectroscopy. Reaction of a toluene solution of a **9** (mixture with **7**) at room temperature under an atmosphere of CO leads within 2 min to the re-formation of **7** in quantitative yield.

Photolysis. Irradiation of toluene solutions of **7b**−**d** with a mercury lamp also leads to the formation of **9b**−**d**. However, this reaction is accompanied by extensive decomposition, probably due to the photolability of **9** on irradiation into the metal−metal bond $\sigma-\sigma^*$ transition (λ = 395 nm), similar to the photodecomposition of the isostructural $Fe_2(CO)_4$(R-ADO).[40]

Thermal and Photochemical Reactivity of $Fe_2(CO)_5(R^1,R^3\text{-ODA})$ (12f−i). Stirring a toluene solution of **12** under an atmosphere of CO at room temperature or at reflux gave no reaction. Refluxing a solution of **12** in toluene under N_2, i.e., without CO, did lead to a new complex (IR) in about 20% yield. However, the new product could not be identified because it decomposed upon purification on silica. Irradiation of **12** in toluene or THF into the high-energy slope of the MLCT band (**12f**; λ = 589 nm) with the 514.5 nm line resulted in slow decomposition, and irradiation with a mercury lamp resulted in fast decomposition of **12f**.

X-ray Structure Determination of 10c and 11b. Orange crystals of **10b** and **11c** suitable for X-ray diffraction were glued to the tip of a Lindemann glass capillary and transferred to an Enraf-Nonius CAD4-F diffractometer in a sealed tube (**10b**) or into the cold nitrogen stream of an CAD4-T diffractometer on a rotating anode (**11c**). Accurate unit-cell parameters and an orientation matrix were determined by least-squares treatment of the setting angles of 22 well-centered reflections (SET4)[44] in the ranges of $8.61° < \theta < 15.32°$ and $9.86° < \theta < 13.83°$ for **10b** and **11c**, respectively. The unit-cell parameters were checked for the presence of higher lattice

(44) Boer, J. L.; Duisenberg, A. J. M. *Acta Crystallogr.* **1984**, *A40*, 410.

Table 2. Crystal Data and Details of the Structure Determination of 10c and 11b

	10c	11b
	Crystal Data	
formula	$C_{16}H_{28}FeN_2O_6$	$C_{13}H_{20}FeN_2O_6$
mol wt	400.25	356.16
cryst syst	monoclinic	monoclinic
space group	$P2_1/c$ (No. 14)	$P2_1/c$ (No. 14)
a (Å)	11.5890(10)	10.0831(6)
b (Å)	19.722(3)	14.7323(11)
c (Å)	10.1620(10)	13.6017(7)
β (deg)	114.950(10)	124.77(5)
V (Å^3)	2105.9(5)	1659.7(10)
Z	4	4
D_{calcd} (g/cm^3)	1.262	1.425
F(000)	848	744
μ(Mo Kα) (cm^{-1})	7.4	9.3
cryst size (mm)	0.30 × 0.25 × 0.30	0.15 × 0.25 × 0.50
	Data Collection	
temp (K)	298	150
θ_{min}, θ_{max} (deg)	1.03, 27.50	1.38, 27.50
wavelength (Mo Kα)(Å)	0.710 73 (Zr filtered)	0.710 73 (graphite monochr)
scan type	$\omega/2\theta$	$\omega/2\theta$
$\Delta\omega$ (deg)	0.53 + 0.35 tan θ	0.59 + 0.35 tan θ
horiz and vert aperture (mm)	3.00, 4.00	3.00, 4.00
X-ray exposure time (s)	73	16
linear decay (%)	2	2
ref rflns	$14\bar{2}$, $\bar{3}2\bar{3}$	$25\bar{3}$, $02\bar{5}$, $12\bar{3}$
data set	−15 to +13, −24 to +13, −10 to +13	−13 to +13, −19 to 0, −17 to +17
total no. of data	5958	8275
total no. of unique data	4820 (R_{int} = 0.030)	3790 (R_{int} = 0.030)
no. of obsd data	1861 ($I > 2.5\sigma(I)$)	3790 (no observn criterion applied)
DIFABS cor range	0.72, 1.10	
	Refinement	
no. of refined params	244	213
final R1[a]	0.054	0.037 (2906, $I > 2\sigma(I)$)
final R_w[b]	0.043	
final wR2[c]		0.086
goodness of fit	1.39	1.01
weighting scheme[d]	$(\sigma^2(F) + 0.000102F^2)^{-1}$	$(\sigma^2(F^2) + (0.0335P)^2)^{-1}$
$(\Delta/\sigma)_{av}$, $(\Delta/\sigma)_{max}$	0.02, 0.08	0.000, −0.003
min and max resid density (e/Å^3)	−0.34, 0.55	−0.44, 0.41

[a] $R1 = \sum||F_o| - |F_c||/\sum|F_o|$. [b] $R_w = [\sum[w(|F_o| - |F_c|)^2]/\sum[w(F_o^2)]]^{1/2}$. [c] $wR2 = [\sum[w(F_o^2 - F_c^2)^2]/\sum[w(F_o^2)^2]]^{1/2}$. [d] $P = (\mathrm{Max}(F_o^2, 0) + 2F_c^2)/3$.

symmetry.[45] Crystal data and details on data collection and refinement are collected in Table 2. Data were corrected for *Lp* effects and for the observed linear decay of the reference reflections. An empirical absorption/extinction correction (DIFABS)[46] was applied for compound **10b**. The structures were solved by automated Patterson methods and subsequent difference Fourier techniques (DIRDIF-92).[47] Refinement on F was carried out by full-matrix least-squares techniques (SHELX76)[48] for **10b**. Compound **11c** was refined on F^2 by full-matrix least-squares techniques (SHELX-93);[49] no observance criterion was applied during refinement on F^2. For both compounds hydrogen atoms were included in the refinement on calculated positions riding on their carrier atoms, except for the amine hydrogen atoms and the C−H hydrogen atoms neighboring an amine moiety, which were located on a difference Fourier map. Their coordinates were included in the refinement. The methyl groups of **11c** were refined as rigid groups, allowing for rotation around the C−C bond. Non-hydrogen atoms were refined with anisotropic displacement parameters. The hydrogen atoms of **10b** were refined with individual isotropic displacement parameters for the freely refined atoms and the hydrogen atoms attached to a tertiary carbon atom. One overall displacement parameter of 0.128(6) Å^2 was applied to all other hydrogens. The hydrogen atoms of **11c** were refined with a fixed isotropic parameter related to the value of the equivalent isotropic displacement parameter of their carrier atoms by a factor amounting to 1.5 for the methyl hydrogen atoms and 1.2 for the other hydrogen atoms, respectively. Compound **10b** was refined using neutral atom scattering factors taken from Cromer and Mann[50] amplified with anomalous dispersion corrections from Cromer and Liberman.[51] For **11c** neutral atom scattering factors and anomalous dispersion corrections were taken from ref 52. Geometrical calculations and illustrations were performed with PLATON;[53] all calculations were performed on a DEC-station 5000 cluster. Additional material available from the Cambridge Crystallographic Data Center comprises H atom coordinates, displacement parameters, and remaining bond lengths and angles.

Table 3. Combinations of Substituents in α-Imino Ester Ligands $R^1N{=}C(H)C(R^3){=}O$ (a−i)

	a	b	c	d	e	f	g	h	i
R^1	*neo*-Pe	*i*-Pr	*i*-Pr	*i*-Pr	CE	*t*-Bu	*t*-Bu	*t*-Bu	*t*-Am
R^3	OMe	OMe	OEt	O-*i*-Pr	OMe	OMe	OEt	O-*i*-Pr	OMe

Results and Discussion

The ligands and complexes discussed are schematically shown in Table 3 and Scheme 3, respectively. The α-imino esters $R^1N{=}C(R^2)C(R^3){=}O$ (R^1 = alkyl, R^2 = H, R^3 = O-alkyl) (L) are indicated by the letters **a**−**i**. The type of complex is identified with Arabic numbers. Reaction of $Fe_2(CO)_9$ with the α-imino esters **a**−**i** at room temperature leads to the formation of several mononuclear and binuclear complexes. The product formation and distribution strongly depend on the nitrogen substituent R^1 and on the solvent.

General Reactions. With all ligands employed the formation of the intense blue (**5f**−**i**) or purple (**5a**−**e**) chelate $Fe(CO)_3$(α-imino ester) complexes is observed. However, complexes **5** are not stable under the reaction conditions and react further with iron carbonyl in toluene and THF to form the $Fe_2(CO)_6$(L) complexes (**6a**−**i**) in low yield (7−16%). Complexes **5** are most likely formed via intermediate **4**, in which the α-imino ester is σ-N coordinated via the nitrogen lone pair to the $Fe(CO)_4$ fragment due to the better σ-donative capacity of nitrogen in comparison to oxygen.[54,55]

Reaction with ligands a−**e**. Reaction of ligands **a**−**e**, i.e., with the less bulky R^1 imine substituents, in toluene leads predominately to the binuclear $Fe_2(CO)_6$-

(45) Spek, A. L. *J. Appl. Crystallogr.* **1988**, *21*, 578.
(46) Walker, N.; Stuart, D. *Acta Crystallogr., Sect. A* **1983**, *A39*, 158.
(47) Beurskens, P. T.; Admiraal, G.; Beurskens, G.; Bosman, W. P.; Garcia-Granda, S.; Gould, R. O.; Smits, J. M. M.; Smykalla, C. The DIRDIF Program System; Technical Report of the Crystallography Laboratory; University of Nijmegen, Nijmegen, The Netherlands, 1992.
(48) Sheldrick, G. M. SHELX76, Crystal Structure Analysis Package; University of Cambridge, Cambridge, England, 1976.
(49) Sheldrick, G. M. SHELXL-93, Program for Crystal Structure Determination; University of Göttingen, Göttingen, Germany, 1993.
(50) Cromer, D. T.; Mann, J. B. *Acta Crystallogr., Sect. A* **1968**, *A24*, 321.
(51) Cromer, D. T.; Liberman, D. *J. Chem. Phys.* **1970**, *53*, 1891.
(52) Wilson, A. J. C. *International Tables for Crystallography*; Kluwer Academic: Dordrecht, The Netherlands, 1992.
(53) Spek, A. L. *Acta Crystallogr., Sect. A* **1990**, *A46*, C34.
(54) Renk, I. W.; tom Dieck, H. *Chem. Ber.* **1972**, *105*, 1403.
(55) Friedel, H.; Renk, I. W.; tom Dieck, H. *J. Organomet. Chem.* **1971**, *26*, 247.

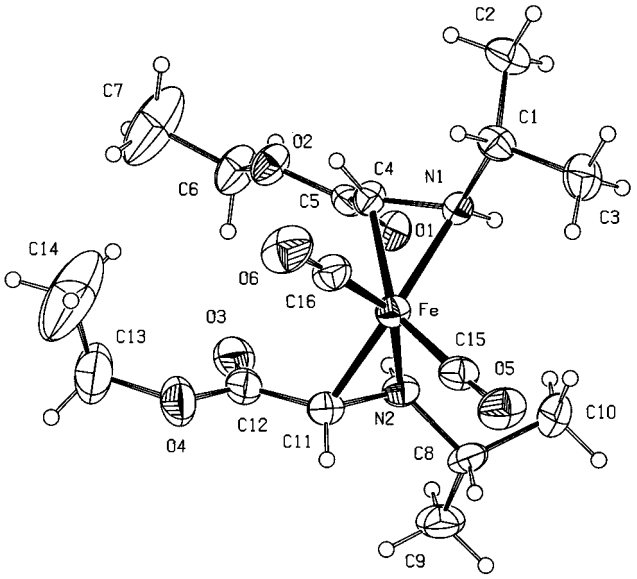

Figure 1. ORTEP drawing (30% probability level) of the molecular structure of **10c**.

(R^1,R^3-ODA)[1] complexes **7a**−**e** in moderate yield (21−25%) together with small amounts (3%) of **10a**−**d**/**10′a**−**d**. In complexes **7a**−**e** the two α-imino ester ligands are reductively coupled via the imine carbon atoms acting as a dianionic six-electron donor. Performing the same reaction in THF leads predominantly to the new mononuclear complexes $Fe(CO)_2(R^1N(H)\text{-}C(H)\text{-}CR^3)_2$ (**10a**−**d**/**10′a**−**d**) in low yield (12−15%) together with small amounts (5%) of **7a**−**d**. In the presence of water, the reaction in THF leads to the formation of $Fe(CO)_2$(*i*-PrN-(H)C(H)-CR^3)(*i*-PrN═C(H)C(O)O) (**11b**,**c**) in 14 and 20% yields, respectively.

Reaction with Ligands f−**i**. With the bulky R^1 imine N-substituted ligands **f**−**i**, a totally different reaction is observed. Reaction in toluene or THF leads to the formation of the new dimeric complexes $Fe_2(CO)_5$-(R^1,R^3-ODA) (**12f**−**i**) in moderate yield (32−38%) or low yield (9−12%), respectively. As in complexes **7**, the newly formed ligand in **12** consists of two α-imino ester ligands which are reductively coupled via the imine carbon atoms. However, in contrast to **7**, both of the C═O oxygen atoms in **12** are coordinated to iron and instead of a metal−metal bond a bridging CO is present. With these ligands complexes **7** and **11** and compound **8** are not observed.

Reaction of complexes **7b**−**e** with aqueous HCl leads to protonation of the bridging aminato nitrogen atoms with formation of the organic products **8b**−**e** in 70% yield. Furthermore, refluxing a toluene solution of **7b**−**d** at 110 °C leads to the loss of two terminal CO ligands under the formation of $Fe_2(CO)_4(R^1,R^3\text{-ODA})$ (**9b**−**d**), in which the C−C coupled ligand is now coordinated with the oxygen of both the ester C═O groups. In the following we will first discuss the structural and spectroscopic data of the relevant complexes and subsequently deal with the aspects of their formation and their reactivity.

Molecular Structure of $Fe(CO)_2$(*i*-PrN(H)C(H)C(O)OEt)$_2$ (10c). An ORTEP view of the molecular structure of **10c** together with the atomic numbering is presented in Figure 1; selected bond distances and angles of **10c** are given in Table 4.

The molecule consists of an Fe(II) center coordinated by two newly formed anionic ligands and two carbonyl ligands. The newly formed ligands are coordinated to iron via both the amine nitrogen and the adjacent carbon atom (η^2(N,C) coordination), thus forming a rather strained three-membered metallacycle. This type of coordination has been observed only a few times with late transition metals.[56] In early-transition-metal chemistry this type of coordination is well-known for many (η^2-pyridyl)$MCp_{1,2}$ (M = Ti, Zr, Y, Sc, Lu) complexes.[57,58]

The nitrogen atoms N(1) and N(2) are donative σ(N) coordinated to iron. The Fe−N(1) (1.983(4) Å) and Fe−N(2) (1.983(5) Å) bond lengths are comparable with the Fe−N(amine) distances reported in the literature.[13,21] The Fe−C(4) (2.045(6) Å) and the Fe−C(11) (1.982(6) Å) distances are shorter than those generally observed for Fe−C(sp^3) (2.07−2.15 Å) bonds.[24,59−62] The shortening of these Fe−C bonds might be due to the coordination of the amine nitrogen, thus bringing the amine carbons C(4) and C(11) closer to the iron center. The amine bond distances (N(1)−C(4) = 1.424(9) Å and N(2)−C(11) = 1.419(9) Å) are somewhat shorter than the mean value of 1.47 Å normally observed for a single N−C(sp^3) bond.[63] The Fe−C(15) and Fe−C(16) bond distances of 1.764(7) and 1.722(7) Å are short for an electron-poor Fe(II) center and indicate extensive π-back-donation toward the carbonyl ligands, which is corroborated by the high-frequency position of the CO resonances in the ^{13}C NMR and the low-frequency position in the IR spectrum. The iron center in **10c** has a strongly distorted tetrahedral coordination geometry, if one considers the two η^2(N,C) coordinated N(1)−C(4) and N(2)−C(11) moieties occupying each one coordination site. While normally an octahedral coordination geometry would be expected for a regular six-coordinate d^6 complex, this rather strange coordination geometry is forced onto the molecule by the η^2(N,C) coordination of the two newly formed ligands.

The crystal structure of **10c** shows a complete intramolecular bifurcated hydrogen bond from N(2) toward O(1) (with N···O = 3.025(6) Å and N−H···O = 143(3)°) and O(3) (with N···O) = 2.799(8) Å and N−H···O = 109(4)°). N(1) is also involved in a bifurcated hydrogen bond toward O(1) (intramolecular, with N···O = 2.873(6) Å and N−H···O = 101(4)°) and O(1) [2 − *x*, −*y*, 1 − *z*] (with N···O = 3.150(7) Å and N−H···O = 156(5)°). The intermolecular hydrogen bond links **10c** into dimers. Both bifurcated hydrogen bonds are nonplanar; the sum of the angles involving the central hydrogen atom amounts to 339(7) and 339(5)° for N(1) and N(2), respectively.

Molecular Structure of $Fe(CO)_2$(σ(*N*):σ(*C*)-*i*-PrNC(H)C(O)OMe)(*i*-PrNC(H)C(O)O) (11b). A view of the

(56) Bouzid, M.; Pradere, J. P.; Palvadeu, P.; Vénien, J. P.; Toupet, L. *J. Organomet. Chem.* **1989**, *369*, 205.
(57) Deelman, B.-J.; Stevels, W. M.; Teuben, J. H.; Lakin, M. T.; Spek, A. L. *Organometallics* **1994**, *13*, 3881.
(58) Thompson, M. E.; Baker, S. M.; Bulls, A. M.; Burger, B. J.; Nolan, C. N.; Santarsiero, B. D.; Schaefer, W. P.; Bercaw, J. E. *J. Am. Chem. Soc.* **1987**, *109*, 203.
(59) Lindner, E.; Schauss, E.; Hiller, W.; Fawzi, R. *Angew. Chem.* **1984**, *96*, 727.
(60) Krüger, C.; Tsay, Y.-H. *Cryst. Struct. Commun.* **1975**, *5*, 215.
(61) Grevels, F.-W.; Feldhoff, U.; Leitich, J.; Krüger, C. *J. Organomet. Chem.* **1974**, 79.
(62) Eilbracht, P.; Jelitte, R.; Walz, L. *Chem. Ber.* **1984**, *117*, 3473.
(63) Ladd, M. F. C.; Palmer, R. A. *Structure Determination by X-ray Crystallography*, 2nd ed.; Plenum Press: New York, 1985.

Table 4. Selected Bond Distances (Å) and Angles (deg) for 10c (Esd's in Parentheses)

Fe−N(1)	1.983(4)	Fe−C(15)	1.764(7)	O(2)−C(5)	1.332(10)	N(2)−C(11)	1.419(9)
Fe−N(2)	1.983(5)	Fe−C(16)	1.722(7)	O(3)−C(12)	1.207(9)	C(4)−C(5)	1.462(9)
Fe−C(4)	2.045(6)	O(1)−C(5)	1.216(9)	O(4)−C(12)	1.346(9)	C(11)−C(12)	1.451(11)
Fe−C(11)	1.982(6)	O(5)−C(15)	1.145(8)	N(1)−C(4)	1.424(9)	O(6)−C(16)	1.158(9)

N(1)−Fe−N(2)	101.8(2)	N(2)−Fe−C(15)	96.6(3)	C(15)−Fe−C(16)	92.1(3)	Fe−C(4)−N(1)	67.0(3)
N(1)−Fe−C(4)	41.4(3)	N(2)−Fe−C(16)	147.5(3)	Fe−N(1)−C(1)	122.8(4)	Fe−C(4)−C(5)	120.5(4)
N(1)−Fe−C(11)	137.5(2)	C(4)−Fe−C(11)	110.4(3)	Fe−N(1)−C(4)	71.6(3)	N(1)−C(4)−C(5)	118.4(6)
N(1)−Fe−C(15)	109.9(3)	C(4)−Fe−C(15)	150.1(3)	C(1)−N(1)−C(4)	118.5(5)	Fe−C(11)−N(2)	69.1(3)
N(1)−Fe−C(16)	104.5(3)	C(4)−Fe−C(16)	89.4(3)	Fe−N(2)−C(8)	125.5(4)	Fe−C(11)−C(12)	116.9(5)
N(2)−Fe−C(4)	98.1(2)	C(11)−Fe−C(15)	98.0(3)	Fe−N(2)−C(11)	69.0(3)	N(2)−C(11)−C(12)	116.0(6)
N(2)−Fe−C(11)	41.9(3)	C(11)−Fe−C(16)	105.9(3)	C(8)−N(2)−C(11)	120.9(5)		

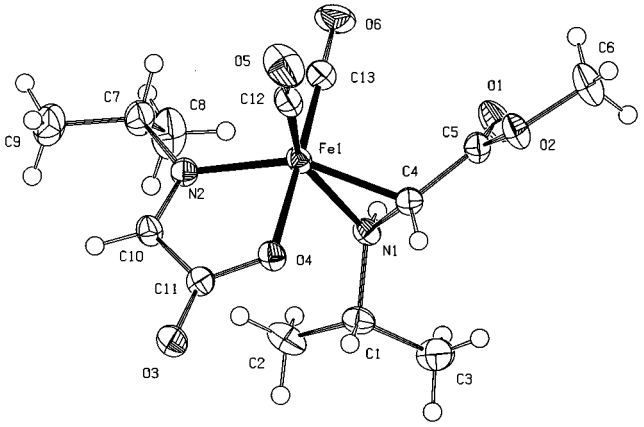

Figure 2. ORTEP drawing (50% probability level) of the molecular structure of **11b**.

molecular structure of **11b** together with the atomic numbering is shown in Figure 2. Selected bond lengths and angles are given in Table 5.

The molecular structure of **11b** consists of an Fe(II) center coordinated by two CO ligands, one η^2(N,C) coordinated ligand as in **10c**, and a newly formed anionic ligand. The intact imine function (N(2)−C(10) = 1.271(3) Å) of the newly formed ligand is coordinated to iron by a normal σ-donative bond Fe(1)−N(2) of 2.0068(17) Å.[14,24,25,32] The bond distances of 1.229(3) and 1.280(3) Å for C(11)−O(3) and C(11)−O(4), respectively, indicate a substantial delocalization within the cyclometalated ester function and compare well with those of Fe[(OC(O)-η^3-allyl)(P(Me)$_3$)$_2$].[64] The Fe(1)−O(4) σ-bond distance of 1.9769(14) Å is consistent with comparable Fe(1)−O−C(O) distances reported in the literature.[32] The carbonyl ligands in **11b** are, as in **10c**, coordinated to iron by relatively short bonds (Fe(1)−C(12) = 1.775(3) Å and Fe(1)−C(13) = 1.762(2) Å); however, these distances are closer to the Fe−CO distances normally observed for Fe(II)−carbonyl ligands. The iron center in **11b** shows a distorted-trigonal-bipyramidal coordination geometry with the η^2(N,C)-coordinated N(1)−C(4) moiety occupying one coordination site. An octahedral coordination geometry, which might be expected for a regular six-coordinate d^6 complex, is not possible due to the η^2(N,C) coordination and the resulting acute N1−Fe(1)−C4 angle of 41.75(12)°. The crystal structure of **11b** shows a bifurcated hydrogen bond from N(1) toward O(1) (intramolecular, with N···O = 2.853(2) Å and N−H···O = 101(2)°) and O(3) [x, $^1/_2 - y$, $-^1/_2 + z$] (with N···O = 2.894(3) Å and N−H···O = 159(2)°); the sum of the angles involving the central hydrogen atom is 359(3)°. The intermolecular hydrogen bond links **11b** into infinite one-dimensional chains parallel to the *c* axis.

IR Spectroscopy. The IR data for the complexes **6a**−**i**, **7a**−**e**, **8b**−**e**, **9b**−**d**, **10a**−**d**/**10′a**−**d**, **11b,c**, and **12f**−**i** are collected in Table 6, together with the FD and FAB mass data and the elemental analyses.

Complexes 6a−**i.** The IR spectra of complexes **6** show five strong terminal carbonyl absorptions in the expected ν(CO) region between 2100 and 1850 cm^{-1}. The pattern of the spectra closely resembles that of the analogous Fe$_2$(CO)$_6$(α-imino ketone)[39,40] and M$_2$(CO)$_6$-(R-DAB) (M = Fe, Ru, Os, FeRu)[16,65−68] complexes. The coordinated ester groups give rise to a weak absorption around 1570 cm^{-1}, a large coordination shift of approximately 160 cm^{-1} to lower frequency. Similar coordination shifts are observed for the analogous Fe$_2$-(CO)$_6$(α-imino ketone) complexes. Coordination of ketone and ester O-donor sites to Fe^{2+}, Fe^{3+} Zn^{2+}, and Al^{3+}[69−72] results in coordination shifts between 50 and 110 cm^{-1}, which are mainly attributed to σ-donation. In Fe(CO)$_3$(α-imino ketone)[25] a very large coordination shift of 200 cm^{-1} is observed, due to σ-donation and extensive π-back-donation from Fe(0) to the antibonding C═O orbital. This suggests that, apart from σ-donation, π-back-donation to the ester moiety also plays an important role in **6**.

Complexes 7a−**e**. Complexes **7** give rise to four or five medium to strong CO stretching bands in the terminal ν(CO) region, and the carbonyl ester functions show two weak absorption bands between 1755 and 1725 cm^{-1}. These latter bands are only marginally shifted compared to those of the free ligands (vide infra), indicating that the ester groups are not involved in coordination toward the iron centers.

Compounds 8b−**e**. The ester carbonyl groups in **8** give rise to one absorption between 1757 and 1744 cm^{-1}: i.e., comparable to those of complexes **7**. The new N−H bond in **8** gives rise to one weak absorption between 3329 and 3336 cm^{-1}, which is indicative of a strong

(64) Hoberg, H.; Jenni, K.; Krüger, C.; Raabe, E. *Angew. Chem., Int. Ed. Engl.* **1986,** *25,* 810.

(65) Staal, L. H.; van Koten, G.; Vrieze, K. *J. Organomet. Chem.* **1981**, *206*, 99.

(66) Zoet, R.; van Koten, G.; Muller, G.; Vrieze, K.; van Wijnkoop, M.; Goubitz, K.; van Halen, C. J. G.; Stam, C. H. *Inorg. Chim. Acta* **1988**, *149*, 193.

(67) Kraakman, M. J.; Elsevier: C. J.; Ernsting, J.-M.; Vrieze, K.; Goubitz, K. *Inorg. Chim. Acta* **1993**, *202*, 129.

(68) Frühauf, H.-W.; Landers, A.; Goddard, R. J.; Krüger, C. *Angew. Chem.* **1978**, *90*, 64.

(69) Torres, M. R.; Santos, A.; Ros, J.; Solans, X. *Organometallics* **1987**, *6*, 1091.

(70) van der Poel, H.; van Koten, G.; Vrieze, K. *Inorg. Chem.* **1980**, *19*, 1145.

(71) van Vliet, M. R. P.; van Koten, G.; Modder, J. F.; van Beek, J. A. M.; Klaver, W. J.; Goubitz, K.; Stam, C. H. *J. Organomet. Chem.* **1987**, *319*, 285.

(72) Lappert, M. F. *J. Chem. Soc.* **1961**, 817.

Table 5. Selected Bond Distances (Å) and Angles (deg) of 11b (Molecule 1, Esd's in Parentheses)

Fe(1)−O(4)	1.9769(14)	Fe(1)−C(13)	1.762(2)	O(4)−C(11)	1.280(3)	N(2)−C(10)	1.271(3)
Fe(1)−N(1)	1.999(2)	O(1)−C(5)	1.205(3)	N(1)−C(1)	1.491(3)	C(4)−C(5)	1.468(3)
Fe(1)−N(2)	2.0068(17)	O(3)−C(11)	1.229(3)	N(1)−C(4)	1.415(3)	C(10)−C(11)	1.500(3)
Fe(1)−C(4)	1.972(2)	O(6)−C(13)	1.146(3)	N(2)−C(7)	1.488(3)	O(5)−C(12)	1.140(4)
Fe(1)−C(12)	1.775(3)						
O(4)−Fe(1)−N(1)	87.29(9)	N(1)−Fe(1)−C(13)	92.89(13)	Fe(1)−N(1)−C(1)	126.53(17)	N(1)−C(4)−C(5)	118.3(2)
O(4)−Fe(1)−N(2)	80.73(9)	N(2)−Fe(1)−C(4)	149.64(12)	Fe(1)−N(1)−C(4)	68.09(16)	O(1)−C(5)−O(2)	123.6(2)
O(4)−Fe(1)−C(4)	86.53(9)	N(2)−Fe(1)−C(12)	99.95(13)	C(1)−N(1)−C(4)	118.69(18)	O(1)−C(5)−C(4)	125.4(2)
O(4)−Fe(1)−C(12)	88.63(11)	N(2)−Fe(1)−C(13)	97.97(11)	Fe(1)−N(2)−C(7)	125.76(17)	O(2)−C(5)−C(4)	111.0(2)
O(4)−Fe(1)−C(13)	178.66(10)	C(4)−Fe(1)−C(12)	107.21(14)	Fe(1)−N(2)−C(10)	113.65(16)	N(2)−C(10)−C(11)	116.1(2)
N(1)−Fe(1)−N(2)	109.78(10)	C(4)−Fe(1)−C(13)	94.49(12)	C(7)−N(2)−C(10)	120.57(19)	O(3)−C(11)−O(4)	126.0(2)
N(1)−Fe(1)−C(4)	41.75(12)	C(12)−Fe(1)−C(13)	91.90(14)	Fe(1)−C(4)−N(1)	70.16(13)	O(3)−C(11)−C(10)	119.9(2)
N(1)−Fe(1)−C(12)	148.88(12)	Fe(1)−O(4)−C(11)	115.46(14)	Fe(1)−C(4)−C(5)	121.31(18)	O(4)−C(11)−C(10)	114.02(19)

Table 6. IR Data[a], Elemental Analyses, and FD/FAB Mass Data[b] of 6,[c] 7,[c] 8,[c] 9,[e] 10/10′,[c] 11,[d] and 12[d]

		elem anal. obsd (calcd) (%)			
compd	IR ν(NH) and ν(CO) (cm^{-1})	C	H	N	M$^+$
6a	2068 s, 2016 vs, 1997 s, 1988 s, 1955 s, 1567 w	38.49 (38.48)	3.46 (3.46)	3.24 (3.21)	
6b	2070 s, 2018 vs, 1998 s, 1987 s, 1955 s, 1572 w	35.32 (35.25)	2.79 (2.71)	3.44 (3.43)	
6c	2068 s, 2018 vs, 1997 s, 1986 s, 1955 s, 1567 w		not anal.		409 (409)
6d	2068 s, 2017 vs, 1996 s, 1985 s, 1954 s, 1560 w		not anal.		437 (437)
6e/6′e	2068 s, 2016 vs, 1997 s, 1985 s, 1954 s, 1568 w		not anal.		477 (477)
6f	2069 s, 2018 vs, 1997 s, 1985 s, 1955 s, 1579 w	36.84 (36.92)	3.19 (3.10)	3.26 (3.31)	
6g	2068 s, 2017 vs, 1996 s, 1985 s, 1954 s, 1574 w		not anal.		437 (437)
6h	2067 s, 2016 vs, 1996 s, 1984 s, 1954 s, 1570 w		not anal.		451 (451)
6i	2068 s, 2017 vs, 1997 s, 1984 s, 1955 s, 1580 w		not anal.		437 (437)
7a	2065 m, 2030 s, 1986 s, 1980 s 1970 m (sh), 1755 w	44.33 (44.47)	5.07 (5.09)	4.66 (4.71)	
7b	2065 m, 2030 s, 1986 s, 1979 s 1969 m (sh), 1754 w, 1741 w	40.29 (40.18)	4.16 (4.12)	5.29 (5.21)	
7c	2065 m, 2031 s, 1986 s, 1978 s, 1749 w, 1733 w	42.32 (42.43)	4.66 (4.63)	4.85 (4.95)	
7d	2065 m, 2030 s, 1986 s, 1977 s, 1744 w, 1725 w		not anal.		594 (594)
7e	2063 m, 2029 s, 1985 s, 1976 s, 1753 w, 1737 w		not anal.		674 (674)
8b	3329 vw, 1744 m		not anal.		261 (260)
8c	3331 vw, 1753 m		not anal.		289 (288)
8d	3332 vw, 1757 m		not anal.		317 (316)
8e	3336 vw, 1754 m				398 (397)
9b	2000 s, 1951 s, 1912 s, 1672 w		not anal.		
9c	1999 s, 1950 s, 1912 s, 1665 w		not anal.		
9d	1997 s, 1948 s, 1910 s, 1658 w		not anal.		538 (538)
10′a	3277 w, 1982 s, 1915 s, 1681 m	50.47 (50.55)	7.54 (7.47)	6.54 (6.59)	428 (428)
10b	3269 w, 3223 w, 1981 s, 1912 s, 1706 m, 1669 m		not anal.		356 (356)
10′b	3243 w, 1981 s, 1912 s, 1689 m		not anal.		356 (356)
10c	3268 w, 3225 w, 1980 s, 1911 s, 1701 m, 1663 m	47.97 (47.97)	7.11 (7.06)	6.83 (7.00)	
10′c	3243 w, 1980 s, 1911 s, 1694 m	47.97 (47.97)	7.11 (7.06)	6.83 (7.00)	
10d	3267 w, 3222 w, 1979 s, 1910 s, 1697 m, 1659 m	50.58 (50.47)	7.60 (7.54)	6.49 (6.54)	
10′d	3244 w, 1979 s, 1912 s, 1679 m	50.58 (50.47)	7.60 (7.54)	6.49 (6.54)	
11b	3273 w, 2022 s, 1956 s, 1699 m, 1661 s	44.06 (43.84)	5.69 (5.66)	7.78 (7.87)	
11c	3271 w, 2021 s, 1955 s, 1693 m, 1661 s	45.59 (45.42)	6.08 (5.99)	7.44 (7.57)	
12f	2022 s, 1975 vs, 1936 s, 1759 w (b), 1700 m	42.35 (42.41)	4.74 (4.87)	5.18 (5.21)	
12g	2021 s, 1974 vs, 1935 s, 1757 w (b), 1696 m	44.68 (44.55)	5.45 (5.34)	4.88 (4.95)	
12h	2022 s, 1974 vs, 1934 s, 1752 w (b), 1687 m		not anal.		594 (594)
12i	2022 s, 1974 vs, 1935 s, 1757 w (b), 1700 m		not anal.		566 (566)
12fg	2022 s, 1974 vs, 1935 s, 1758 w (b), 1697 m		not anal.		

[a] Abbreviations: vs = very strong, s = strong, m = medium, w = weak, vw = very weak, sh = shoulder, b = broad. [b] Observed (calculated) FD masses of molecular ion M$^+$ (*m*/*e*) of complexes **6**, **7**, and **9**−**12**; M$^+$ values are based upon ^{56}Fe isotope; observed (calculated) FAB masses of molecular ion M$^+$ (*m*/*e*) of **8**. [c] IR measured in pentane. [d] IR measured in dichloromethane. [e] IR measured in toluene, derived from mixture of **7** and **9**.

N−H bond. This is also evident from the low-frequency position of the N−H protons in the ^{1}H NMR (see below). Hydrolysis of EtZn[*t*-BuNC(H)C(NEt$_2$)═O]$_2$, an N,N′-bridged C−C coupled dimer of the closely related α-imino amide *t*-BuN═C(H)C(NEt$_2$)═O, results in the N-protonated organic compound 1,2-bis(*N*,*N*-diethylcarbonamide)-1,2-bis(*tert*-butylamine)ethane.[73] The N−H absorption of this compound is found at somewhat lower frequency (3280 cm^{-1}).

Complexes 9b−d. The IR spectra of complexes **9** show three terminal CO stretching bands around 1998, 1948, and 1910 cm^{-1}. The ester carbonyls give rise to a weak band at about 1665 cm^{-1}, a shift of ca. 80 cm^{-1} to lower wavenumber compared to those of **7**, which indicates Fe−O═C coordination. The pattern and position of the observed CO stretching bands strongly resemble those of Fe$_2$(CO)$_4$(R-ADO), suggesting that complexes **9** are structurally analogous.

Complexes 10a−d/10′a−d and 11b,c. The symmetric and antisymmetric CO stretching bands (A$_1$, B$_2$) of dicarbonyl−Fe(II) complexes are normally found at or somewhat below 2040 cm^{-1} (A$_1$) and 1980 cm^{-1} (B$_2$).[27,31,74] The two intense CO stretching bands of complexes **11** are found at clearly lower frequencies

(73) Van Vliet, M. R. P. Ph.D. Thesis, University of Amsterdam, 1987.

(74) Breuer, J.; Frühauf, H.-W.; Smeets, W. J. J.; Spek, A. L. *Inorg. Chim. Acta* **1999**, *291*, 438.

(around 2020 and 1956 cm^{-1}), but those of complexes **10** are found at extremely low wavenumbers of about 1980 and 1912 cm^{-1}. They indicate extensive π-back-donation to the terminal carbonyls. From this one has to infer a very strong donor capacity of the three-electron-donating C−N fragments (σ(C), κ-(N)). In addition, the unusual coordination geometries (vide supra), i.e., close to trigonal bipyramidal (**11**) and tetrahedral (**10**), may also play a role.

As expected, the ester carbonyl groups in the symmetric complexes **10′a**−**d** give rise to only one stretching band at about 1685 cm^{-1}, and those in the asymmetric complexes **10b**−**d** give rise to two bands around 1700 and 1665 cm^{-1}. The ester carbonyl stretching bands of complexes **11** are found at 1695 cm^{-1}. The bands are shifted between 30 and 70 cm^{-1} to lower wavenumber compared to those of the free ligand. These rather pronounced shifts are ascribed to the presence of intramolecular hydrogen bridges with the newly formed N−H bonds, evident from the X-ray structures of **10c** and **11b**, and to the anionic character of the ligand. The cyclometalated ester carbonyl in **11** gives rise to a strong carbonyl stretching band at 1661 cm^{-1}. The new N−H bonds in the symmetric complexes **10′** give rise to one and those in the asymmetric complexes **10** to two absorption bands in the ν(N−H) region between 3222 and 3277 cm^{-1}. The N−H vibration of complexes **11** is found at 3272 cm^{-1}. These absorptions are generally somewhat lower than the ν(N−H) absorptions (3275−3305 cm^{-1}) observed for $FeM(CO)_6$[RNC(R)C(R)N(**H**)R] (M = Mn, Re) and $Ru_2(CO)_6$[RCC(H)C(H)N(**H**)R].[15,75]

Complexes 12f−**i**. The IR spectra of complexes **12** give rise to three terminal CO stretching bands around 2022, 1974, and 1935 cm^{-1}. The bridging carbonyl ligands give rise to a weak and broad absorption band around 1755 cm^{-1}. The pattern of these CO stretching bands strongly resembles that of $Ru_2(CO)_5$(R-ADA),[1] a similarly C−C coupled dimer of R-DAB.[10,16] This makes it reasonable to assume similar structures; i.e., the oxygen atoms of the two C═O ester groups in **12** are coordinated to the iron centers. The coordinated ester groups give rise to an absorption band between 1700 and 1687 cm^{-1}, a coordination shift of 40 cm^{-1}. This small shift in comparison with the coordination shift of 160 cm^{-1} in **6** suggests that in **12** the ester C═O donor sites act purely as a σ-donor.

NMR Spectroscopy. The ^{1}H and ^{13}C NMR data of complexes **6**, **7**, **8**, **9**, **10/10′**, **11/11′**, and **12** are collected in Tables 7 and 8, respectively.

Complexes 6. The ^{1}H and ^{13}C resonances of the imine protons and the imine carbon atoms of complexes **6** are observed between 3.58 and 3.29 and 55.4−48.9 ppm, respectively. These shifts are typical for μ_2(N),η^2-(C═N) coordination of the C═N moiety and agree with those found in $M_2(CO)_6$(R-DAB or R-Pyca)[16,65−67] and $Fe_2(CO)_6$(α-imino ketone).[39,40] The carboxyl carbon atoms show coordination shifts of 25−28 ppm to higher frequency, indicating that the Fe−O bond still mainly consists of σ(O) donation (see IR Spectroscopy).

Since the α-imino ester is asymmetrically coordinated, the six terminal carbonyl ligands in complexes **6** are inequivalent and should in a rigid metal carbonyl skeleton give rise to six independent resonances. However, complexes **6** show only one signal at room temperature, while at 243 K three separate signals are observed. The signal at room temperature does not lie at the weighted average ppm value of the signals at 243 K. This indicates local scrambling of the carbonyl groups of one iron center at 243 K, while the carbonyl ligands on the other iron center are in the limit of slow exchange. A similar dynamic behavior has been reported for $Fe_2(CO)_6$(R-DAB)[76] and $Fe_2(CO)_6$(α-imino ketone).[40] Individual assignment of CO resonances to either one of the two $Fe(CO)_3$ moieties can be deduced from carbonyl resonances of $FeRu(CO)_6$(R-Pyca),[67] in which the μ_2(N),η^2(C═N) coordination of the C═N moiety is directed to iron. In the ^{13}CO NMR of these complexes recorded at 263 K the Fe−carbonyl ligands appear as one signal, while the Ru−carbonyl ligands give rise to three separate resonances. On this basis, the three CO resonances observed at 243 K correspond to the μ_2(N),σ-(O) coordinated $Fe^1(CO)_3$ center and the resonance observed at room temperature to the three CO ligands on the μ_2(N),η^2(C═N) coordinated $Fe^2(CO)_3$ moiety (cf. Scheme 3).

For ligand **e**, containing a chiral 1-cyclohexylethyl substituent on nitrogen, the two diastereomeric complexes **6e** and **6′e** are formed in a 3:1 ratio due to the imine carbon, which becomes chiral upon η^2(C═N) coordination. For **6e/6′e** dynamic behavior is observed to be similar to that for the other complexes **6**.

Complexes 7. The ^{1}H and ^{13}C resonances of the former imine protons and imine carbon atoms, observed between 3.67 and 3.81 and 72.8−73.5 ppm, respectively, are shifted ca. 4 and 80 ppm to lower frequency in comparison with those in the free ligand. This clearly shows that the former imine functions are reductively coupled via the imine carbon atoms; i.e., they are now sp^3 hybridized, resulting in two anionic aminato nitrogen donor sites. The carboxyl carbon atoms of the noncoordinating ester groups resonate around 172 ppm, a coordination shift of ca. 11 ppm to higher frequency compared to those of the free ligand. However, these δ values are still normal for ester carboxyl carbon atoms and compare well with those observed in compounds **8b**−**e**.

Compounds 8b−**e**. The central carbon atoms appear around 41.0 (**8b**−**d**) and 42.7 (**8e**) ppm, respectively. The shift of ca. 25−30 ppm to lower frequency compared to the corresponding carbon atoms in complexes **7** is a result of the protonation of the bridging anionic aminato nitrogen atoms. The new N−H protons in compounds **8b**−**e** resonate between 1.81 and 1.52 ppm. This is at relatively low frequency and is indicative of an electron-rich, strong N−H bond, consistent with the IR data. The large ^3J coupling in **8d** between the N−H and the central C−H proton (^3J = 9.7 Hz) indicates that the N−H and C−H bonds are nearly coplanar. The dihedral angle between the N−H bond and the *i*-Pr C−H bond is probably close to 90°, as can be concluded from the ^3J coupling of only 1.9 Hz (Karplus−Conroy relation) between these protons. In **8b**,**c**,**e**, however, the N−H

(75) Mul, W. P.; Elsevier: C. J.; van Leijen, M.; Vrieze, K.; Smeets, W. J. J.; Spek, A. L. *Organometallics* **1992**, *11*, 1877.

(76) Staal, L. H.; Keijsper, J.; Polm, L.; Vrieze, K. *J. Organomet. Chem.* **1981**, *204*, 101.

Table 7. ^{1}H NMR Data[a] of Complexes 6, 7, 9, 10/10′,[b] 11/11′, and 12

compd	δ
6a	3.91, 3.50 (2 × 1H, d, 13.0 Hz, NC*H*H), 3.58 (3H, s, OCH_3), 3.56 (1H, s, N=C*H*), 1.26 (9H, s, $CH_2(CH_3)_3$)
6b	3.56 (3H, s, OCH_3), 3.55 (1H, sept, 6.4 Hz, C*H*$(CH_3)_2$), 3.36 (1H, s, N=C*H*), 1.63, 1.54 (2 × 3H, d, 6.4 Hz, CH(CH_3)$_2$)
6c	3.98, 3.92 (2 × 1H, dq, 10.8 Hz, 6.8 Hz, OC*H*H), 3.54 (1H, sept, 6.0 Hz, C*H*$(CH_3)_2$), 3.33 (1H, s, N=C*H*), 1.62, 1.54 (2 × 3H, d, 6.4 Hz, CH(CH_3)$_2$), 1.20 (3H, t, 6.8 Hz, CH_2CH_3)
6d	4.61 (1H, sept, 6.1 Hz, O-*i*-Pr C*H*), 3.52 (1H, sept, 6.2 Hz, N-*i*-Pr C*H*), 3.29 (1H, s, N=C*H*), 1.61, 1.52 (2 × 3H, d, 6.2 Hz, *i*-Pr CH_3), 1.17, 1.15 (2 × 3H, d, 6.1 Hz, *i*-Pr CH_3)
6e	3.58 (3H, s, OCH_3), 3.56 (1H, s, N=C*H*), 2.47 (1H, m, *c*-Hex C*H*), 1.86−1.10 (10H, m, *c*-Hex CH_2), 1.32 (3H, d, 6.9 Hz, CH(CH_3))
6′e	3.59 (3H, s, OCH_3), 3.34 (1H, s, N=C*H*), 2.75 (1H, m, *c*-Hex C*H*), 1.86−1.10 (10H, m, *c*-Hex CH_2), 1.44 (3H, d, 6.9 Hz, CH(CH_3))
6f	3.57 (1H, s, N=C*H*), 3.32 (3H, s, OCH_3), 1.48 (9H, s, C(CH_3)$_3$)
6g	4.02, 3.92 (2 × 1H, dq, 10.8 Hz, 7.1 Hz, OC*H*H), 3.31 (1H, s, N=C*H*), 1,21 (3H, t, 7.1 Hz, CH_2CH_3), 1.47 (9H, s, C(CH_3)$_3$)
6h	4.63 (1H, sept, 6.2 Hz, *i*-Pr C*H*), 3.28 (1H, s, N=C*H*), 1.47 (9H, s, C(CH_3)$_3$), 1.19, 1.17 (2 × 3H, d, 6.2 Hz, *i*-Pr CH_3)
6i	3.57 (3H, s, OCH_3), 3.35 (1H, s, N=C*H*), 2.01, 1.77 (2 × 1H, dq, 13.4 Hz, 7.4 Hz, C*H*HCH$_3$), 1.33, 1.32 (2 × 3H, s, C(CH_3)$_2$), 1.08 (3H, t, 7.4 Hz, CH_2CH_3)
7a	3.77 (6H, s, 2 × OCH_3), 3.67 (2H, s, 2 × N−C*H*), 3.10, 2.80 (2 × 2H, d, 14.5 Hz, 4 × NCH*H*), 0.97 (18H, s, 2 × $CH_2(CH_3)_3$)
7b	3.81 (2H, s, 2 × N−C*H*), 3.72 (6H, s, 2 × OCH_3), 3.25 (2H, sept, 6.8 Hz, 2 × N-*i*-Pr C*H*), 1.49, 1.08 (2 × 6H, d, 6.8 Hz, 4 × *i*-Pr CH_3)
7c	4.21, 4.14 (2 × 2H, dq, 11 Hz, 7.1 Hz, 4 × OC*H*H), 3.77 (2H, s, 2 × N−C*H*), 3.25 (2H, sept, 6.8 Hz, 2 × *i*-Pr C*H*), 1.49, 1.11 (2 × 6H, d, 6.8 Hz, 4 × *i*-Pr CH_3), 1.28 (6H, t, 7.1 Hz, 2 × CH_2CH_3)
7d	5.05 (2H, sept, 6.3 Hz, 2 × O*i*-Pr−C*H*), 3.72 (2H, s, 2 × N−C*H*), 3.24 (2H, sept, 6.8 Hz, 2 × N-*i*-Pr C*H*), 1.49, 1.13 (2 × 6H, d, 6.8 Hz, 4 × N-*i*-Pr CH_3), 1.27, 1.21 (2 × 6H, d, 6.3 Hz, 4 × O-*i*-Pr CH_3),
7e	3.87 (6H, s, 2 × OCH_3), 3.73 (2H, s, 2 × N−C*H*), 2.79 (2H, dq, 12.8, 6.9 Hz, 2 × C*H*(CH_3)), 2.06 (2H, m, *c*-Hex C*H*), 1.75−0.70 (20H, m, *c*-Hex CH_2), 1.45 (6H, d, 6.9 Hz, 2 × CH(CH_3))
8b	3.74 (6H, s, 2 × OCH_3), 3.70 (2H, s, 2 × NC*H*), 2.67 (2H, sept, 6.2 Hz, 2 × *i*-Pr C*H*), 1.79 (2H, s, b, 2 × N*H*), 1.03, 0.88 (2 × 6H, d, 6.2 Hz, 4 × *i*-Pr CH_3)
8c	4.19 (4H, q, 7.2 Hz, 2 × OCH_2), 3.69 (2H, s, 2 × NC*H*), 3.24 (2H, sept, 6.2 Hz, 2 × *i*-Pr C*H*), 1.81 (2H, s, b, 2 × N*H*), 1.30 (6H, t, 7.2 Hz, 2 × CH_2CH_3), 1.03, 0.89 (2 × 6H, d, 6.2 Hz, 4 × *i*-Pr CH_3)
8d	5.05 (2H, sept, 6.3 Hz, 2 × O-*i*-Pr C*H*), 3.62 (2H, d, 9.7 Hz, 2 × NC*H*), 2.65 (2H, dsept, 6.1, 1.9 Hz, 2 × N-*i*-Pr C*H*), 1.75 (2H, br d, 9.7 Hz, 1.9 Hz, 2 × N*H*), 1.28, 1.26 (2 × 6H, d, 6.3 Hz, 2 × O-*i*-Pr CH_3), 1.01, 0.90 (2 × 6H, d, 6.1 Hz, 2 × N-*i*-Pr CH_3)
8e	3.73 (6H, s, 2 × OCH_3), 3.71 (2H, s, 2 × NC*H*), 1.52 (2H, br s, 2 × N*H*), 1.74−1.53 (16H, m, *c*-Hex *H*, C*H*(CH_3)), 1.26−1.06 (10H, m, *c*-Hex *H*), 0.94 (6H, d, 6.6 Hz, 2 × CH(CH_3))
9b	4.49 (2H, s, 2 × N−C*H*), 3.79 (6H, s, 2 × OCH_3), 3.49 (2H, sept, 6.8 Hz, 2 × N-*i*-Pr C*H*), 1.18, 1.07 (2 × 6H, d, 6.8 Hz, 4 × *i*-Pr CH_3)
10′a	3.96 (2H, d, 7 Hz, 2 × NC*H*), 3.76 (6H, s, 2 × OCH_3), 2.45 (2H, d, 13.1 Hz, 2 × NC*H*H), 2.14 (2H, pt, 11.1, 7 Hz, 2 × N*H*), 1.89 (2H, dd, 13.1, 11.1 Hz, 2 × NCH*H*), 0.94 (18H, s, 2 × $CH_2(CH_3)_3$)
10b	3.82 (3H, s, OCH_3), 3.46 (1H, d, 5.3 Hz, NCH), 3.46 (3H, s, OCH_3), 2.87 (1H, d, 7.9 Hz, NCH), 2.76 (1H, br, dd, 8.6, 7.9 Hz, NH), 2.71 (1H, br dd, 10.0, 5.3 Hz, NH), 1.91 (1H, ds, 7.1, 8.6 Hz, *i*-Pr CH), 1.71 (1H, ds, 10.0, 6.4 Hz, *i*-Pr CH), 1.02, 0.82 (2 × 3H, d, 6.4 Hz, *i*-Pr CH_3), 0.92, 0.67 (2 × 3H, d, 7.1 Hz, *i*-Pr CH_3)
10′b	3.73 (2H, d, 7.1 Hz, 2 × NC*H*), 3.45 (6H, s, 2 × OCH_3), 2.13 (2H, br pt, 10.9, 7.1 Hz, 2 × N*H*), 1.64 (2H, ds, 10.9, 6.6 Hz, 2 × *i*-Pr C*H*), 0.89, 0.70 (2 × 6H, d, 6.4Hz, 4 × *i*-Pr CH_3)
10c	4.53, 4.33, 4.27, 3.94 (4 × 1H, dq, 10.7, 6.3 Hz, OC*H*H), 3.53 (1H, d, 7.4 Hz, NC*H*), 2.85 (1H, d, 7.8 Hz, NC*H*), 2.78 (1H, br, dd, 9.6, 7.8 Hz, N*H*), 2.75 (1H, br, dd, 10.7, 7.4 Hz, N*H*), 1.91 (1H, ds, 10.7, 6.3 Hz, *i*-Pr C*H*), 1.73 (1H, ds, 11.6, 6.3 Hz, *i*-Pr C*H*), 1.24, 1.18 (2 × 3H, t, 7.1Hz, CH_2CH_3), 1.03, 0.93, 0.81, 0.69 (4 × 3H, d, 6.3Hz, *i*-Pr CH_3)
10′c	4.20, 3.94 (2 × 2H, dq, 10.8, 7.2 Hz, 4 × OC*H*H), 3.74 (2H, d, 7.1 Hz, 2 × NC*H*), 2.21 (2H, br dd, 10.8, 7.2 Hz, 2 × N*H*), 1.68 (2H, ds, 10.7, 6.3 Hz, 2 × *i*-Pr C*H*), 1.08 (6H, t, 7.2 Hz, 2 × CH_2CH_3), 0.95, 0.74 (2 × 6H, d, 6.3 Hz, 4 × *i*-Pr CH_3)
10d	5.38 (1H, sept, 6.4 Hz, *i*-Pr C*H*), 5.11 (1H, sept, 6.4 Hz, *i*-Pr C*H*), 3.52 (1H, d, 7.4 Hz, NC*H*), 2.85 (1H, br pt, 11.5, 7.4 Hz, N*H*), 2.72 (1H, br pt, 10.7, 7.7 Hz, N*H*), 2.71 (1H, d, 7.7 Hz, NC*H*), 1.92 (1H, ds, 9.5, 6.4 Hz, *i*-Pr C*H*), 1.75 (1H, ds, 10.7, 6.4 Hz, *i*-Pr C*H*), 1.46, 1.36, 1.30, 1.19, 1.03, 0.93, 0.82, 0.70 (10 × 3H, d, 6.4 Hz, *i*-Pr CH_3)
10′d	5.08 (2H, sept, 6.3 Hz, 2 × *i*-Pr C*H*), 3.69 (2H, d, 7.2 Hz, 2 × NC*H*), 2.23 (2H, br pt, 10.4, 7.2 Hz, 2 × N*H*), 1.69 (2H, ds, 10.4, 6.3 Hz, 2 × *i*-Pr C*H*), 1.20, 1.15, 0.97, 0.75 (4 × 6H, d, 6.3 Hz, 10 × *i*-Pr CH_3)
11b	7.77 (1H, s, N=C*H*), 4.31 (1H, sept, 6.5 Hz, *i*-Pr C*H*), 4.00 (1H, d, 8.8 Hz, NC*H*), 3.74 (3H, s, OCH_3), 3.51 (1H, br dd, 11.0, 8.8 Hz, N*H*), 2.85 (1H, ds, 11, 6.6 Hz, *i*-Pr C*H*), 1.53, 1.52 (2 × 3H, d, 6.5Hz, *i*-Pr CH_3), 1.26, 1.01 (2 × 3H, d, 6.6Hz, *i*-Pr CH_3)
11′b[c]	7.79 (1H, s, N=C*H*), 4.31 (1H, sept, 6.3 Hz, *i*-Pr C*H*), 3.80 (3H, s, OCH_3), 3.63 (1H, d, 10.4 Hz, NC*H*), 3.15 (1H, br dd, 10.5, 10.4 Hz, N*H*), 2.49 (1H, ds, 10.5, 6.6 Hz, *i*-Pr C*H*), 1.51, 1.40 (2 × 3H, d, 6.3Hz, *i*-Pr CH_3), 1.26, 1.01 (2 × 3H, d, 6.6Hz, *i*-Pr CH_3)
11c	7.77 (1H, s, N=C*H*), 4.33 (1H, sept, 6.7 Hz, *i*-Pr C*H*), 4.31, 4.14 (2 × 1H, dq, 10.9, 7.3 Hz, OC*H*H), 4.05 (1H, d, 10.9 Hz, NC*H*), 3.40 (1H, br dd, 10.9, 8.9 Hz, N*H*), 2.88 (1H, ds, 10.9, 6.5 Hz, *i*-Pr C*H*), 1.55, 1.54, 1.28, 1.02 (2 × 3H, d, 6.5 Hz, *i*-Pr CH_3), 1.29 (3H, t, 6.7 Hz, CH_2CH_3)
12f	3.81 (6H, s, 2 × OCH_3), 3.50 (2H, s, 2 × N−C*H*), 1.83, (6H, s, b, 2 × C(CH_3), 1.27 (2 × 12H, br s, 4 × C(CH_3)) (1.82, 1.29, 1.20)
12g	4.29, 4.22 (2 × 2H, dq, 10.9 Hz, 7.1 Hz, 4 × OC*H*H), 3.45 (2H, s, 2 × N−C*H*), 1.83, (6H, br s, 2 × C(CH_3)),, 1.32 (2 × 6H, br s, 4 × C(CH_3)), 1.31 (6H, t, 7.1 Hz, 2 × CH_2CH_3) (1.79, 1.27, 1.18)
12h	5.00 (2H, sept, 6.2 Hz, 2 × *i*-Pr C*H*), 3.36 (2H, s, 2 × N−C*H*), 1.82 (6H br s, 2 × C(CH_3)), 1.28 (12H, s, br s, 4 × C(CH_3)), 1.30, 1.28 (2 × 6H, d, 6.2 Hz, 4 × *i*-Pr CH_3) (1.711, 1.26, 1.18)
12i	3.80 (6H, s, 2 × OCH_3), 3.58 (2H, s, 2 × NC*H*), 1.71 (6H, s, b, 2 × C(CH_3), 1.68 (1H, m, b, C*H*HCH$_3$), 1.52 (2H, m, b, CH_2CH_3), 1.33 (1H, m, b, C*H*HCH$_3$), 1.18 (6H, s, b, 2 × C(CH_3)) 1.00 (6H, t, b, 2 × CH_2CH_3)
12fg	4.28, 4.22 (2 × 1H, dq, 10.7 Hz, 6.8 Hz, OCH_2), 3.81 (3H, s, OCH_3), 3.48, 3.46 (2 × 1H, d, 10.6 Hz, N−C*H*), 1.83 (6H, br s, 2 × C(CH_3)), 1.31 (12H, br s, 4 × C(CH_3), 1.31 (3H, t, 7.1 Hz, CH_2CH_3)

[a] Abbreviations: s = singlet, d = doublet, t = triplet, q = quartet, dq = double quartet, sept = septet, ds = double septet, dd = double double. δ values are in ppm relative to TMS, measured in $CDCl_3$ at 293 K and 300.13 MHz. [b] Measured in C_6D_6 at 293 K and 300.13 MHz. [c] Derived from a mixture.

Table 8. ^{13}C NMR Data[a] of Complexes 6,[b] 7, 8, 9, 10/10′, 11/11′, and 12[d]

compd	δ
6a	216.2, (213.2), 212.5, 201.7 (*C*O), 185.4 (*C*═O), 81.7 (NCH_2), 59.0 (OCH_3), 55.4 (*C*═N), 36.0 (*C*$(CH_3)_3$), 29.5 (C(CH_3)$_3$)
6b	216.4, (213.8), 211.0, 201.8 (*C*O), 187.1 (*C*═O), 66.3 (*i*-Pr *C*H), 55.2 (OCH_3), 52.1 (*C*═N), 28.1, 27.2 (*i*-Pr *C*H_3)
6c	216.6, (213.4), 211.0, 201.9, (*C*O), 186.7 (*C*═O), 66.3 (*i*-Pr-*C*H), 64.7 (OCH_2), 52.5 (*C*═N), 28.2, 27.1 (*i*-Pr-*C*H_3), 14.5 (OCH_2*C*H_3)
6d	216.7, (213.9), 211.1, 202.1 (*C*O), 186.7 (*C*═O), 73.1 (*i*-Pr O*C*H), 66.3 (*i*-Pr N*C*H), 52.9 (*C*═N), 28.2, 27.1, 22.1, 21.8 (*i*-Pr *C*H_3)
6e[d]	216.2, (214.0), 211.5, 202.1 (*C*O), 185.7 (*C*═O), 73.6 (N*C*H(CH_3)), 55.3 (OCH_3), 49.8 (*C*═N), 32.8 (*c*-Hex *C*H), 27.5, 27.0, 26.7, 25.7 (*c*-Hex *C*H_2), 18.1 (CH(*C*H_3))
6′e[d]	216.2, (214.0), 211.5, 202.1 (*C*O), 186.5 (*C*═O), 75.7 (N*C*H(CH_3)), 50.8 (OCH_3), 49.4 (*C*═N), 32.3 (*c*-Hex *C*H), 27.5, 27.0, 26.7, 25.7 (*c*-Hex *C*H_2), 18.1 (CH(*C*H_3))
6f	216.6, (214.2), 210.7, 201.8 (*C*O), 188.1 (*C*═O), 64.0 (*C*$(CH_3)_3$), 55.7 (OCH_3), 48.9 (*C*═N), 33.7 (C(CH_3)$_3$)
6g	216.8, (214.3), 210.7, 201.9 (*C*O), 187.1 (*C*═O), 64.7 (OCH_2), 64.0 (*C*$(CH_3)_3$), 49.2 (*C*═N), 33.3 (C(CH_3)$_3$), 14.6 (OCH_2*C*H_3)
6h	217.0, (214.3), 210.8, 201.9 (*C*O), 187.3 (*C*═O), 73.1 (O*C*H), 64.0 (*C*$(CH_3)_3$), 49.5 (*C*═N), 33.6 (C(CH_3)$_3$), 22.1, 21.8 CH(*C*H_3)$_2$)
6i	216.7, (214.3), 210.7, 201.6 (*C*O), 188.0 (*C*═O), 66.6 (N*C*), 55.2 (OCH_3), 49.2 (*C*═N), 40.4 (*C*H_2CH$_3$), 31.2, 29.0 (C(CH_3)$_2$), 11.5 (CH_2*C*H_3)
7a	213.3, 212.6, 204.3 (*C*O), 170.4 (*C*═O), 76.1 (N*C*H_2), 73.5 (N*C*H), 52.8 (OCH_3), 35.1 (*C*$(CH_3)_3$), 30.4 (C(CH_3)$_3$)
7b	213.2, 212.2, 204.1 (*C*O), 173.2 (*C*═O), 72.8 (N*C*H), 67.6 (*i*-Pr *C*H), 53.2 (OCH_3), 26.2, 23.8 (*i*-Pr *C*H_3)
7c	213.4, 212.3, 204.2 (*C*O), 173.0 (*C*═O), 73.2 (N*C*H), 67.7 (*i*-Pr *C*H), 62.4 (OCH_2), 26.6, 22.9 (*i*-Pr *C*H_3), 14.6 (OCH_2*C*H_3)
7d	213.4, 212.3, 204.2 (*C*O), 172.7 (*C*═O), 73.5 (N*C*H), 69.8 (*i*-Pr O*C*H), 67.7 (*i*-Pr N*C*H), 26.7, 24.0, 22.4, 22.0 (*i*-Pr *C*H_3)
7e	213.4, 212.1, 204.1 (*C*O), 173.1 (*C*═O), 77.6 (N*C*H(CH_3)), 73.4 (N*C*H), 52.9 (OCH_3), 45.9 (*c*-Hex *C*H), 34.0, 32.2, 27.7, 27.0, 26.8 (*c*-Hex *C*H_2), 22.3 (NCH(*C*H_3))
8b	174.4 (*C*═O), 62.3 (*i*-Pr *C*H), 52.7 (OCH_3), 48.4 (N*C*H), 24.2, 22.8 (*i*-Pr *C*H_3)
8c	173.9 (*C*═O), 62.4 (*i*-Pr *C*H), 61.7 (OCH_2), 48.4 (N*C*H), 24.2, 22.9 (*i*-Pr *C*H_3), 15.0 (OCH_2*C*H_3)
8d	173.4 (*C*═O), 69.3 (O-*i*-Pr *C*H), 62.3 (N-*i*-Pr *C*H), 48.4 (N*C*H), 24.2, 23.1, 22.7, 22.5 (*i*-Pr *C*H_3)
8e	174.6 (*C*═O), 63.6 (N*C*HCH$_3$), 58.1 (OCH_3), 42.7 (N*C*H), 2 × 27.6, 27.5, 27.3 (*c*-Hex *C*H_2)), 17.6 (NCH*C*H_3)
9b	212.6, 212.5 (*C*O), 181.3 (*C*═O), 63.9 (N*C*H), 61.6 (*i*-Pr *C*H), 56.1 (OCH_3), 22.8, 22.2 (*i*-Pr *C*H_3)
10a	218.8 (*C*O), 178.8 (*C*═O), 68.7 (N*C*H_2), 52.5 (OCH_3), 49.1 (N*C*H), 33.9 (*C*$(CH_3)_3$), 28.1 (C(CH_3)$_3$)
10b	218.5, 215.5 (*C*O), 178.8, 177.3 (*C*═O), 59.4, 59.2 (*i*-Pr *C*H), 52.4, 52.3 (OCH_3), 42.7, 41.3 (N*C*H), 25.3, 25.0, 23.1, 23.0 (*i*-Pr *C*H_3)
10′b	219.3 (*C*O), 178.8 (*C*═O), 59.3 (*i*-Pr *C*H), 52.5 (OCH_3), 44.3 (N*C*H), 25.6, 21.3 (*i*-Pr *C*H_3)
10c	218.7, 215.7 (*C*O), 178.1, 176.9 (*C*═O), 61.3, 60.8 (OCH_2CH$_3$), 2 × 59.1 (*i*-Pr *C*H), 43.5, 41.5 (N*C*H), 25.2, 24.9, 23.0, 22.9 (*i*-Pr *C*H_3), 14.9, 14.8 (OCH_2*C*H_3)
10′c	219.2 (*C*O), 179.2 (*C*═O), 61.1 (OCH_2CH$_3$), 59.1 (*i*-Pr *C*H), 43.3 (N*C*H), 25.5, 21.7 (*i*-Pr *C*H_3), 15.0 (OCH_2*C*H_3)
10d	218.9, 215.8 (*C*O), 177.4, 176.7 (*C*═O), 69.1, 67.8 (*i*-Pr O*C*H), 2 × 59.0 (*i*-Pr N*C*H), 44.3, 41.7 (N*C*H), 25.1, 24.8, 3 × 23.0, 22.7, 22.4, 21.9 (*i*-Pr *C*H_3)
10′d	219.5 (*C*O), 179.0 (*C*═O), 68.2 (*i*-Pr O*C*H), 59.3 (*i*-Pr N*C*H), 44.7 (N*C*H), 25.6, 23.0, 22.6, 21.4 (*i*-Pr *C*H_3)
11b	211.7, 211.2 (*C*O), 177.4, 171.4 (*C*═O), 163.3 (N═*C*H), 64.3 (*i*-Pr *C*H), 53.2 (OCH_3), 48.8, 48.7 (N*C*H; *i*-Pr *C*H), 24.8, 24.1, 23.4, 23.0 (*i*-Pr *C*H_3)
11′b[d]	212.7, 211.6 (*C*O), 174.8, 172.0 (*C*═O), 163.7 (N═*C*H), 64.0 (*i*-Pr *C*H), 56.7 (OCH_3), 52.9, 46.9 (N*C*H; *i*-Pr *C*H), 24.9, 24.3, 23.0, 22.7 (*i*-Pr *C*H_3)
11c	211.8, 211.2 (*C*O), 176.8, 171.4 (*C*═O), 163.2 (N═*C*H), 64.5 (*i*-Pr *C*H), 61.9 (OCH_2CH$_3$), 49.5, 48.7 (N*C*H; *i*-Pr *C*H), 24.8, 24.0, 23.4, 22.6 (*i*-Pr *C*H_3), 14.8 (OCH_2*C*H_3)
12f	258.6 (bridging *C*O), 212.8, 210.9 (*C*O), 183.2 (*C*═O), 66.4 (N*C*H), 60.1 (*C*$(CH_3)_3$), 55.8 (OCH_3), 34.7, 31.4, 29.3 (3 × CCH_3)
12g	258.9 (bridging *C*O), 213.0, 211.0 (*C*O), 182.7 (*C*═O), 66.7 (N*C*H), 65.1 (OCH_2), 60.1 (*C*$(CH_3)_3$), 34.8, 31.6, 29.4 (3 × CCH_3), 14.6 (OCH_2*C*H_3)
12h	261.3 (bridging *C*O), 213.0, 211.0 (*C*O), 182.2 (*C*═O), 73.4 (*i*-Pr *C*H), 66.7 (N*C*H), 60.0 (*C*$(CH_3)_3$), 34.7, 31.6, 29.3 (3 × CCH_3), 22.1, 21.0 (*i*-Pr *C*H_3)
12i	258.9, 258.2 (bridging *C*O), 213.1, 212.9, 210.9, 210.5 (*C*O), 183.6, 183.3, 183.0, 182.7 (*C*═O), 66.3, 65.8, 65.7 (3 × N*C*H), 63.2, 62.8, 62.6 (3 × *C*$(CH_3)_3$), 55.7 (OCH_3), 38.0, 36.9, 34.0 (3 × *C*H_2CH$_3$), 30.8, 30.7, 28.1, 27.9, 25.8, 24.7 (6 × NCCH_3), 12.0, 11.7, 11.4 (3 × CH_2*C*H_3)

[a] δ values in ppm relative to TMS, measured in $CDCl_3$ at 263 K and 75.47 MHz. [b] Measured at 243 K, ppm value in parentheses measured at 293 K. [c] Measured at 293 K. [d] Measured at 243 K.

resonances appear as a broad singlet, indicating that in these compounds the N−H bond, the *i*-Pr C−H (**8b**,**c**) or C_5H_{10} C−H (**8e**) bond, and the central C−H bond are nearly orthogonal. The observation that in **8d** the N−H proton couples with both the *i*-Pr C−H and less so with the proton on the central carbon is probably due to the increased bulkiness of the isopropyl ester, forcing **8d** into a different conformation than **8b**,**c**,**e**.

Complex 9c. The ester carboxyl carbon atom resonances (181.3 ppm) of **9c** are shifted ca. 10 ppm to higher frequency compared to those in **7c**. The positions of these resonances compare well with those observed for the corresponding carbon atoms in **12**, indicating Fe−O═C coordination. The four terminal CO ligands are observed as two closely spaced resonances at ca. 212.6 ppm: i.e., analogous to the resonances observed for the CO ligands in the isostructural $Fe_2(CO)_4$(R-ADO).[40]

Complexes 10a−d/10′a−d. The ^{1}H NMR spectra of complexes **10** are reported in benzene-d_6 because of considerable overlap of the signals in $CDCl_3$. As expected, the symmetric complexes **10′a−d** show, both in their ^{1}H and ^{13}C NMR spectra, only one set of signals, while the asymmetric complexes **10b−d** give rise to two separate sets of signals. The N−H protons in **10′a** show a large ^3J coupling with one of the diastereotopic methylene protons of the neopentyl group (11.1 Hz) and in **10b−d/10′b−d** with the isopropyl methine proton (ca. 12 Hz). Also, the additional ^3J coupling with the proton on the metalated carbon atom is relatively large (ca. 7

Hz). This indicates that the N−H bond is almost coplanar with one of the methylene C−H bonds (**10′a**) or the isopropyl methine C−H bond (**10b**−**d**/**10′b**−**d**) and with the metalated C−H bond, which is consistent with the solid-state structure of **10b** (i.e., dihedral angles of 175(4)° (HC(1)−N(1)−H) and 151(5)° (HC(4)−N(1)−H)). For a formal Fe(II) complex, the resonances of the terminal carbonyl carbon atoms are observed at rather low field (219.3−215.5 ppm), indicating a large degree of π-back-donation. The cyclometalated carbon atoms in complexes **10**/**10′** resonate between 49 and 41 ppm: i.e., normal ppm values for sp^3-cyclometalated carbon atoms.[59]

Complexes 11b,c. The imine protons and the imine carbon atom resonances of complexes **11** are observed between 7.77 and 7.71 ppm and at ca. 163 ppm; i.e., no significant coordination shift is observed. This indicates that the coordination of the imine consists mainly of σ-(N) donation, which is also evident from the C=N bond length of 1.271(3) Å in the solid-state structure of **11b**. The N−H proton in **11b**,**c**/**11′b**,**c** gives rise to a broad double doublet (pseudotriplet) at 3.51 and 3.15 ppm, respectively. Analogously to complexes **10**, the N−H protons show large coupling constants with both the isopropyl methine proton (10 Hz) and the proton (10 Hz) on the cyclometalated carbon atom. When **11c** is synthesized in the presence of D_2O instead of H_2O, the signal is reduced to approximately 70% of its normal intensity in the ^{1}H NMR spectrum, while in the ^{2}H NMR spectrum a weak signal at 3.1 ppm is observed, which proves that the proton on nitrogen originates from water. The reduction of the signal by only 30% is probably due to reexchange of deuterium for hydrogen during workup on silica gel. The terminal carbonyls of complexes **11** resonate between 213 and 211 ppm, a shift of ca. 4 ppm to lower frequency in comparison with those in complexes **10**, reflecting a decrease in π-back-donation which is also observed in the IR data.

The ^{1}H NMR of **11b**, measured immediately after column chromatography, revealed that a second isomer was present **11′b**, in approximately 6% yield. The given ^{1}H and ^{13}C spectral data of **11′b** are derived from this mixture.

Complexes 12. The ^{1}H NMR spectra of complexes **12** show at room temperature very broad resonances for the *t*-Bu and *t*-Am substituents on nitrogen, indicating that rotation around the N−C bond is hindered, probably due to interaction with the bridging carbonyl. Cooling solutions of complexes **12f**−**h** to 243 K results in three separate sharp signals for the tert-butyl methyl groups, showing that at this temperature the rotation of the *t*-Bu group is frozen in. The limit of fast exchange could not be reached due to some decomposition at 363 K: i.e., formation of paramagnetic species. As a result of the hindered rotation around the N−C bond, complex **12i** (*t*-Am) is present as distinguishable isomers. The ^{13}C NMR clearly shows three sets of resonances in approximately a 1:3:5 ratio, and in the proton spectra three isomers can also be distinguished, although the assignment is difficult due to overlap of the signals. Just as in complexes **7**, the former imine protons and imine carbon atoms are shifted to lower frequency by ca. 3.3 and 80 ppm, respectively, showing that the former imine carbon atoms are reductively coupled. The bridging carbonyl ligand resonances are observed between 258 and 261 ppm, which are normal ppm values for bridging CO ligands.[77] The resonances of the coordinated carboxyl carbon atoms are observed at ca. 182−183 ppm: i.e., a high-frequency coordination shift of approximately 20 ppm compared to those of the free ligand, indicating that the ester C=O donor sites are coordinated and act as σ-donors.

Scheme 4. Proposed Reaction Mechanism for the Formation of 6

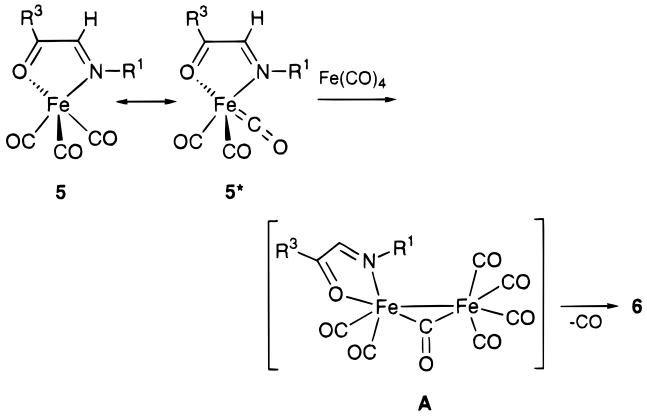

Complex Formation/Reactions of α-Imino Esters with Carbonyliron. The formation of the complexes described above depends strongly on the imine nitrogen R^1 substituent and the solvent. In the following we will discuss the possible mechanisms for the formation of complexes **6**−**12** and their reactivity.

Formation of $Fe(CO)_3$(α-imino ester) (5). Reaction of the α-imino esters **a**−**i** with $Fe_2(CO)_9$ at room temperature in toluene or THF leads initially to the formation of the monodentate N-coordinated intermediate $Fe(CO)_4[N(R^1)=C(H)C(R^3)=O]$ (**4**), as result of the better σ-coordinating properties of nitrogen compared with oxygen[54,55] (cf. Scheme 3). With all ligands, intermediate **4** reacts further to complexes **5**: i.e., CO substitution and coordination of the ester carbonyl. The formation of the chelate complexes is indicated by the deep purple (**5a**−**e**) or deep blue (**5f**−**i**) reaction mixtures, analogous to the intensely colored $Fe(CO)_3$(R-DAB) and $Fe(CO)_3$(α-imino ketone) complexes. Unfortunately, however, complexes **5** could not be isolated due to their instability and reactivity, resulting in the formation of complexes **6** and **12**. The existence of complexes **5** has been proven by in situ 1,3-dipolar cycloaddition reactions of **5** with DMAD, resulting in $Fe(CO)_3$(butenolide) complexes,[35] analogous to the formation of complexes **3** (cf. Scheme 1: X = O; R^1 = *n*-Pr, *i*-Pr, *t*-Bu, *t*-Am; R^3 = OMe, OEt, O-*i*-Pr).

Formation of $Fe_2(CO)_6$(α-imino ester) (6a−i). Further reaction of $Fe(CO)_3$(α-imino ester) (**5**) with $Fe(CO)_4$ in THF, toluene, or pentane results in the formation of the known type of binuclear $Fe_2(CO)_6$(α-imino ester) complexes **6** (cf. Scheme 4).

Complexes **6** are probably formed via a binuclear CO-bridged intermediate (A). A similar intermediate has been proposed for the formation of $Fe_2(CO)_6$(R-DAB)[78] and $Fe_2(CO)_6$(α-imino ketone).[40] The formation of A can

(77) Frühauf, H.-W. *J. Chem. Res., Miniprint* **1983**, 2035.
(78) Frühauf, H.-W.; Breuer, J. *J. Organomet. Chem.* **1984**, *277*, C13.

be described as isolobally related[79,80] to the addition of a carbene to an olefin giving a cyclopropane ring system; i.e., in the present case $Fe(CO)_4$ is isolobal with a carbene and adds to the Fe═C double bond (isolobal with an olefin) in resonance structure **5***, which results in the formation of intermediate A. Subsequent π-coordination of the C═N double bond, i.e., formation of the μ_2(N),η^2(C═N) bridge, with concomitant extrusion of CO results in the formation of complexes **6**. Complexes **6** are isolated as red-brown slightly air-sensitive crystalline solids. The α-imino esters in complexes **6** are μ_2-(N),σ(O):η^2(C═N) coordinated to the two iron centers and donate six electrons, analogous to the coordination of α-imino ketones in $Fe_2(CO)_6$(α-imino ketone).[39,40] Complexes **6** are formed in low yields and in general the yields decrease somewhat on going from ligand **a** via **b**−**e** to ligands **f**−**i**. This is in agreement with the decreasing propensity for η^2(C═N) coordination on increasing bulkiness of the R^1-imine nitrogen substituent, **a** (RCH_2), **b**−**e** (R_2CH), **f**−**i** (R_3C), a trend also observed for R-DAB[81] and α-imino ketones.[40] The yields of complexes **6** in THF and toluene are almost identical, while the reaction in pentane leads to slightly lower yields. With chiral ligand **e** two diastereomeric complexes **6e** and **6e′** are formed in a 3:1 ratio due to the imine carbon, which becomes chiral upon η^2-C═N coordination.

Reactivity of Complexes 6. Complexes **6** do not react thermally or photochemically with an excess of free ligand. Consequently, we can exclude **6** as an intermediate in the formation of the binuclear complexes **7** and **12**. Furthermore, complexes **6** do not react with activated alkynes such as DMAD. This is in contrast with the rich chemistry of $M_2(CO)_6$(R-DAB) (M = Fe, Ru) with activated alkynes and other unsaturated substrates, leading to many interesting C−C (Ru) and C−N (Fe) coupled products.[19,21,82] Reaction of complexes **6** with CO (1−50 atm) at room temperature or at elevated temperatures, leads to decomposition of **6**, and the monomeric complexes **5** are not detected, as is the case for $Fe_2(CO)_6$(R-DAB).[83] The η^2(C═N) coordination is probably stronger than the σ(O) coordination, and as a result, the coordinated oxygen atom is substituted by CO, which triggers the decomposition of **6**.

Formation of $Fe_2(CO)_6(R^1,R^3$-ODA) (7a−e) and $Fe_2(CO)_5(R^1,R^3$-ODA) (12f−i). When heated at reflux (120 °C) or irradiated in toluene at room temperature, complexes **7b**−**d** lose two CO ligands with exclusive formation of **9b**−**d** (cf. Scheme 5) and complexes **12b**−**d** are not detected. Furthermore, complexes **12f**−**i** do not react to the corresponding complexes **7f**−**i** when heated to 110 °C in toluene under an atmosphere of CO (1 bar). Refluxing a toluene solution of **12f**−**i** under N_2 leads to decomposition (see Experimental Section), without formation of the corresponding complexes **9f**−**i**: i.e., loss of CO in **12**. The latter reaction has been reported for $Ru_2(CO)_5$(R-ADA) (R = *t*-Bu, *i*-Pr, *p*-Tol, *c*-Hex),[10] resulting in $Ru_2(CO)_4$(R-ADA). For R = *t*-Bu, this reaction proceeds only photochemically in good yield. Irradiation of **12f**−**i**, however, leads to decomposition of **12f**−**i** and complexes **9f**−**i** are not observed.

Scheme 5. Observed Interconversions of 7, 9, and 12

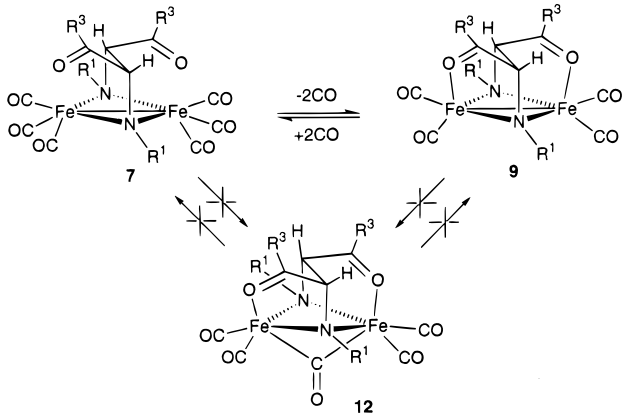

The different reactivities show that complexes **7** and **12** are most likely formed via different reaction paths, although they contain the same C−C coupled ligand. Complexes **7** are exclusively formed with the less bulky R^1-substituted ligands **a**−**e,** and complexes **12** are exclusively formed with the more bulky R^1-substituted ligands **f**−**i**. Apparently, the R^1 substituent has a decisive influence on the involved intermediates, thus giving rise to the observed product selectivity.

Upon reaction of the bulky N−R^1 substituted ligands **f**−**i** with $Fe_2(CO)_9$ the reaction mixture becomes colored more quickly and much more intensely than with the less bulky N−R^1 substituted ligands **a**−**e**. This is indicative of a faster formation, and of higher concentrations, of the chelate complexes **5f**−**i** in comparison with **5a**−**e**. This is also reflected in the much higher yields obtained for the in situ 1,3-dipolar cycloaddition reaction of **5f**−**i** (54−68%) than for **5a**−**d** (18−30%).[35] The faster reaction from **4** to **5** (chelation) for ligands **f**−**i** can possibly be explained by steric interactions. From the crystal structure of $Fe(CO)_4$[MeN═C(H)C(H)═C(H)Ph] [84] it is known that the *N*-methyl substituent interacts sterically with one of the equatorial CO ligands. For the bulky N−R^1 substituted ligands **f**−**i** this will lead to even stronger interactions between the equatorial CO ligands and the R^1 substituent, forcing the ester carbonyl toward the iron, thus resulting in a faster reaction to the chelate complexes **5f**−**i**.

Formation and Structure of 12. The fast formation of the chelate complexes **5f**−**i** results in high stationary concentrations of **5f**−**i**, and the fact that the carbonyl ester functions are coordinated in **12f**−**i** strongly points to a reaction mechanism in which the chelate complex **5** plays an important role. Therefore, complexes **12** are suggested to be formed via intermediate B, similar to the proposed reaction mechanisms for the formation of the isostructural $Ru_2(CO)_{4,5}$(R-ADA)[10] and $Fe_2(CO)_4$(R-ADO)[40] (cf. Scheme 6). Just as for the formation of intermediate A (cf. Scheme 4), the formation of intermediate B can be seen as an isolobal analogue to the reaction between a carbene and an olefin. In the present case, dissociation of one of the terminal CO ligands in

(79) Hoffmann, R. *Science* **1981**, *211*, 995.
(80) Hoffmann, R. *Angew. Chem.* **1982**, *94*, 725.
(81) Staal, L. H.; Polm, L.; Vrieze, K.; Ploeger, F.; Stam, C. H. *Inorg. Chem.* **1981**, *20*, 3590.
(82) Staal, L. H.; van Koten, G.; Vrieze, K.; van Santen, B.; Stam, C. H. *Inorg. Chem.* **1981**, *20*, 3598.
(83) Frühauf, H.-W.; Wolmershäuser, G. *Chem. Ber.* **1982**, *115*, 1070.
(84) Nesmeyanov, A. N.; Rybin, L. V.; Stelzer, N. A.; Struchkov, Y. T.; Batsanov, A. S.; Rybinskaya, M. I. *J. Organomet. Chem.* **1979**, *182*, 399.

Scheme 6. Proposed Reaction Mechanism for the Formation of 12

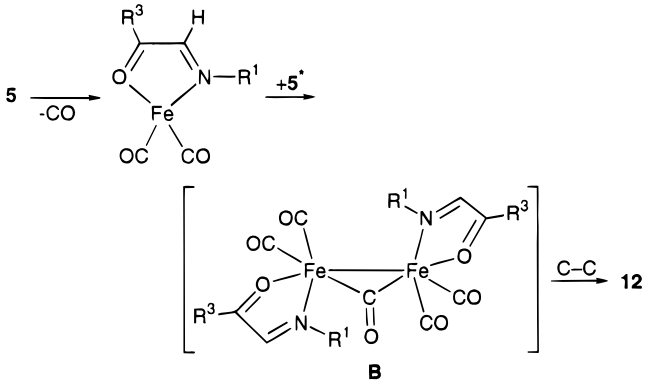

Scheme 7. Possible Mechanism for the Formation of 7

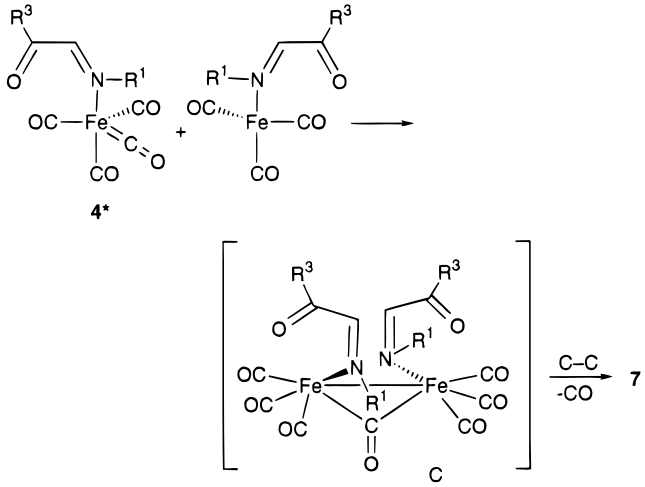

5f−**i** leads to $Fe(CO)_2$(α-imino ester), a d^8 ML_4 fragment like $Fe(CO)_4$ and thus isolobal with a carbene. Subsequent addition to the Fe═C bond in **5*** (isolobal with an olefin; Scheme 4) gives intermediate B, in which, in contrast to intermediate A, two σ(N):σ(O) coordinated α-imino ester ligands are present. Reductive C−C coupling of the imine carbons results, after breakage of the metal−metal bond, in the formation of **12**.

Though it is rather unusual to have a bridging carbonyl between two formally unbonded metal atoms, we are fairly confident in the structure of **12** as shown in Scheme 3 for the following reasons. The X-ray diffraction data sets of two measured (twinned) complexes **12** do confirm the topology, which was based on the IR and NMR spectroscopic data, and indicate an Fe−Fe bond length of 2.60 Å. This is indeed a distance normally found for bonding interactions. However, in the isostructural complex $Ru_2(CO)_4$(R-ADA),[10] which also has the CO-bridged ruthenium atoms at a normally bonding distance of 2.873(2) Å, it could be shown by temperature-dependent UV−vis spectroscopy that no direct metal−metal bond is present.

Interestingly, with the ligands **a**−**e** complexes **12a**−**e** are not formed while the mononuclear chelate complexes **5a**−**e** are definitely present, although in lower stationary concentrations. Apparently, a high concentration of the chelate **5** is necessary to induce the formation of **12**. This is in agreement with the observation that $Fe_2(CO)_5$(*c*-Hex-DAB)$_2$, i.e., isostructural to intermediate B, is only formed at rather high concentrations of $Fe(CO)_3$(*c*-Hex-DAB)[85] upon irradiation (λ < 488 nm) in pentane at 150 K, while at low concentrations decomposition is observed. Furthermore, this explains the lower yields observed for the formation of **12** in toluene; i.e., due to the limited solubility of $Fe_2(CO)_9$ in toluene compared to THF, lower concentrations of **5f**−**i** are produced and accordingly complexes **12** are formed in low yield. Upon heating, $Fe_2(CO)_5$(*c*-Hex-DAB)$_2$ reacts back to $Fe(CO)_3$(*c*-Hex-DAB), indicating that in this case the imine carbon atoms are apparently not sufficiently activated to undergo C−C coupling.

Formation of 7. Complexes **7a**−**e** are most likely formed starting from the monodentate N-coordinated α-imino ester intermediate complex **4**, which has, like **7**, a pendant ester moiety. It is, however, difficult to propose a mechanism for the formation of **7a**−**e**, because no intermediates can be observed. Complexes **7** could, in line with the proposed mechanisms for the formation of **6** and **12**, be formed via a similar type of reaction mechanism (cf. Scheme 7). In this case, $Fe(CO)_3$[(R^1)N═C(H)−C(R^3)═O] (d^8 ML_4 fragment) is isolobal with a carbene and adds to the Fe═C double bond (isolobal with an olefin) in resonance structure **4***, which results in the formation of intermediate C.

During the formation of complexes **7** the two prochiral imine carbon atoms become chiral centers. De Cian et al.[39] have shown that the chiral centers are coupled and only the *R*,*R* and *S*,*S* combinations are formed. Likewise, reaction with ligand **e**, bearing a chiral (*R*)-cyclohexylethyl substituent on nitrogen, may lead to two diastereoisomers, only one of which is observed. Similar high diastereomeric ratios are obtained with *N*-cyclohexylethyl-substituted ligands in 1,3-dipolar cycloadditions.[86]

Formation of $Fe(CO)_2(R^1N(H)C(H)C(O)R^3)_2$ (10a−**d/10′a**−**d)**. Complexes **10** are formed in low yield on reaction of the α-imino esters **a**−**d** with $Fe_2(CO)_9$ at room temperature in THF. In toluene **10** is formed only in traces (3%), and when pentane is used as a solvent, it is not observed. It is obvious that some electron-transfer step has taken place and the imine double bond has been hydrogenated, presumably by hydrogen abstraction from the solvent, because the yields parallel the hydrogen donor properties of the solvent.[87,88] To confirm this, a small-scale reaction was carried out in THF-d_8 (1 mL). The result of this experiment tends to support the assumption that THF is the hydrogen donor, since the N−H resonance in the ^{1}H NMR spectrum is reduced to 80% of the intensity, although reservations have to be made because considerable line broadening hampered the interpretation. The partial exchange of deuterium for a proton on nitrogen is probably caused by workup on silica gel.

Like complexes **7**, complexes **10** are only formed with the less bulky ligands **a**−**d**. Therefore, they are probably

(85) van Dijk, H. K.; Stufkens, D. J.; Oskam, A. *J. Am. Chem. Soc.* **1989**, *111*, 541.

(86) Feiken, N.; Schreuder, P.; Siebenlist, R.; Frühauf, H.-W.; Vrieze, K.; Kooijman, H.; Veldman, N.; Spek, A. L.; Fraanje, J.; Goubitz, K. *Organometallics* **1996**, *15*, 2169.

(87) van Wijnkoop, M. Ph.D. Thesis, University of Amsterdam, 1992.

(88) Kidd, D. R.; Cheng, D. P.; Brown, T. L. *J. Am. Chem. Soc.* **1978**, *100*, 4103.

also formed via intermediate **4**. However, it is unknown via which mechanism complexes **10** are formed, except that at some stage of the reaction an electron-transfer step is involved.

Complexes **10** are obtained as two isomers, an asymmetric (**10**) and a symmetric (**10′**) isomer, in a ratio of ca. 6:1 except for **10′a**, which is formed as the symmetric isomer exclusively. The ratio of the two isomers does not change on heating to 60 °C, while further heating results in decomposition. The observation that with ligand **a** exclusively the symmetric isomer is formed, and with the ligands **b**−**d** the asymmetric isomer is favored, has to be ascribed to the steric requirements of the substituent R^1 on nitrogen. In the symmetric complex the ester group of one of the ligands and the nitrogen R^1 substituent of the other ligand are pointing toward each other; i.e., they sterically interact. For the neopentyl-substituted ligand **a** this interaction will be minimal because the neopentyl group can easily bend away. For the more bulky isopropyl-substituted ligands **b**−**d**, however, the steric interaction is apparently such that they preferentially form the asymmetric complexes **10b**−**d**.

Complexes **10/10′** are isolated as yellow powders and are slightly air sensitive in crystalline form. Reaction of **10/10′** with H_2O results in decomposition, and formation of **11** is not observed. Complexes **10** do not insert unsaturated molecules such as alkenes or alkynes into the strained M−C bond, as is observed for the (η^2-pyridyl)$MCp_{1,2}$ (M = Ti, Zr, Y, Sc, Lu) complexes.[57,58]

Formation of $Fe(CO)_2(\sigma(N):\sigma(C)$-$R^1NC(H)C(O)$-$R^3)(R^1N{=}C(H)C(O)O)$ (11). Reaction of the α-imino esters **b** and **c** with $Fe_2(CO)_9$ at room temperature in THF in the presence of H_2O leads to the formation of **11b/11′b** (12:1) and **11c** in 14 and 20% yields, respectively. Since there are no observable intermediates, a detailed reaction mechanism cannot be given. However, it is plausible that **11** is formed via a route similar to that for **10**, with H_2O in this case as hydrogen donor. This was confirmed by the reaction with D_2O (see NMR Spectroscopy).

Comparison of Different Iron Carbonyl/1,4-Diheteroatom-1,3-butadiene Systems in C−C Coupling Reactions. We have shown above that with α-imino esters C−C coupling is only observed between the imine carbon atoms of two α-imino esters. For the closely related α-imino ketones $R^1N{=}C(H)C(R^3){=}O$ and C_5H_4N-2-$C(R^3){=}O$ (R^1 = *t*-Bu, *t*-Am; R^3 = Me, Ph), however, exclusive coupling of the methyl-substituted ketone carbon atoms is observed.[40] In the case of R-DAB and R-Pyca, C−C coupling is not observed at all for Fe, while for Ru[9,10,18] these types of C−C coupling reactions occur readily, resulting in either $Ru_2(CO)_{4,5}$(R-ADA) or $Ru_2(CO)_{4,5}$(R-APE).[1]

The observation that the α-imino ketones exclusively couple on the methyl-substituted ketone-C atoms is in line with the 1,3-dipolar reactivity of the chelate $Fe(CO)_3$(α-imino ketone); i.e., exclusive addition over the Fe−O=C fragment is observed. From this it might be concluded that the reactivities for 1,3-dipolar cycloadditions and the C−C coupling reactions discussed here are possibly determined by the same factors. This is corroborated by the enhanced reactivity of $Ru(CO)_3$(R-DAB) in both 1,3-dipolar cycloaddition[23] and C−C coupling reactions. In both types of reactions, steric interactions also play an important role. When one of the two imine C atoms in R-DAB bears a methyl substituent, $R^1N{=}C(Me)C(H){=}NR^1$, either type of reaction exclusively takes place at the unsubstituted imine carbon atom.

The observation that with the α-imino ketones $R^1N{=}C(H)C(Ph){=}O$ C−C coupling of the ketone-C atoms is not observed is probably due to electronic reasons as well as steric reasons. It is known that the 1,3-dipolar reactivity of the ketone carbon atom in $Fe(CO)_3$(α-imino ketone) is lowered on substitution with an electron-withdrawing substituent (R^3 = Ph vs Me).[89,90] Therefore, the introduction of the electron-withdrawing alkoxy substituents (R^3 = O-alkyl) on the ketone carbon atom might be the reason for the change in reactivity of α-imino esters compared to that of α-imino ketones: i.e., coupling of the imine or ketone carbon atoms. This is corroborated by the in situ cycloaddition reactions of **5a**−**i**, which result in cycloaddition across both the Fe−O=C and Fe−N=C fragments. [35] It must be emphasized, however, that the Fe−O=C fragment is still more reactive in this case. Furthermore, steric interactions of the O-alkyl substituents could prevent C−C coupling of the carboxyl carbon atoms.

However, why in the case of iron C−C coupling of the imine-C atoms is not observed for R-DAB, R-Pyca, and $R^1N{=}C(H)C(Ph){=}O$ is not clear. Apparently, the imine carbon atoms in these systems are not activated sufficiently for C−C coupling, whereas they are in the α-imino ester system.

Acknowledgment. The investigation was supported in part (A.L.S.) by The Netherlands Foundation for Chemical Research (SON) with financial aid from The Netherlands Organization for Scientific Research (NWO).

Supporting Information Available: Listings of crystallographic data for the structure determinations of compounds **10c** and **11b**, including final coordinates of non-hydrogen atoms, hydrogen atom positions, (an)isotropic thermal parameters, bond distances and angles, and torsion angles. This material is available free of charge via the Internet at http://pubs.acs.org.

OM9910266

(89) Houk, K. N.; Sims, J.; Watts, C. R.; Luskus, L. J. *J. Am. Chem. Soc.* **1973**, *95*, 7301.
(90) Houk, K. N.; Sims, J.; Duke, R. E.; Strozier, R. W.; George, J. K. *J. Am. Chem. Soc.* **1973**, *95*, 7287.